DIE ERDE **142** 2011 (3)	Contributions to Geoarchaeology	pp. 259-288

• *Olympia – Tsunami events – Beachrock – Peloponnese*

Andreas Vött, Georg Bareth, Helmut Brückner, Franziska Lang, Dimitris Sakellariou, Hanna Hadler, Konstantin Ntageretzis and **Timo Willershäuser**

Olympia's Harbour Site Pheia (Elis, Western Peloponnese, Greece) Destroyed by Tsunami Impact

Die Zerstörung von Olympias Hafen Pheia (Elis, Westpeloponnes, Griechenland) durch Tsunami-Impakt

With 5 Figures, 1 Table and 2 Photos

It is well known from historic catalogues that the Greek coast has repeatedly been struck by large earthquakes and associated tsunami events during the past millennia. The seismically highly active Hellenic Arc, where the African plate is being subducted by the Aegean microplate, is considered to be the most significant tsunami source in the wider region. The study presented in this paper focuses on sedimentary and geomorphological tsunami traces encountered at Pheia, western Peloponnese (Greece), one of the harbours of the nearby cult site Olympia. Sedimentological, pedological, geoarchaeological and geochemical analyses revealed tsunami sand and gravel of mostly marine origin reaching far inland. Wave refraction and channeling effects seem to have steepened tsunami waters up to 18-20 m above present sea level and induced tsunami water passage across the narrow Katakolo Pass into adjacent coastal plains. Tsunami deposits that were accumulated onshore were partly cemented and later exposed in the form of beachrock. By radiocarbon dating and archaeological age estimation of ceramic fragments, three distinct tsunami events were found, namely for the 6th millennium BC, for the time around 4300 ± 200 cal BC and for the Byzantine to post-Byzantine period. Olympia's harbour site Pheia was finally destroyed by tsunami landfall, most probably in the 6th century AD and accompanied by co-seismic submergence.

1. Introduction

From earthquake and tsunami catalogues it is well known that the eastern Mediterranean has been struck by numerous strong tsunami impacts since ancient times. These events destroyed coastal settlements and infrastructure and caused thousands of fatalities (*Guidoboni* et al. 1994, *Tinti*

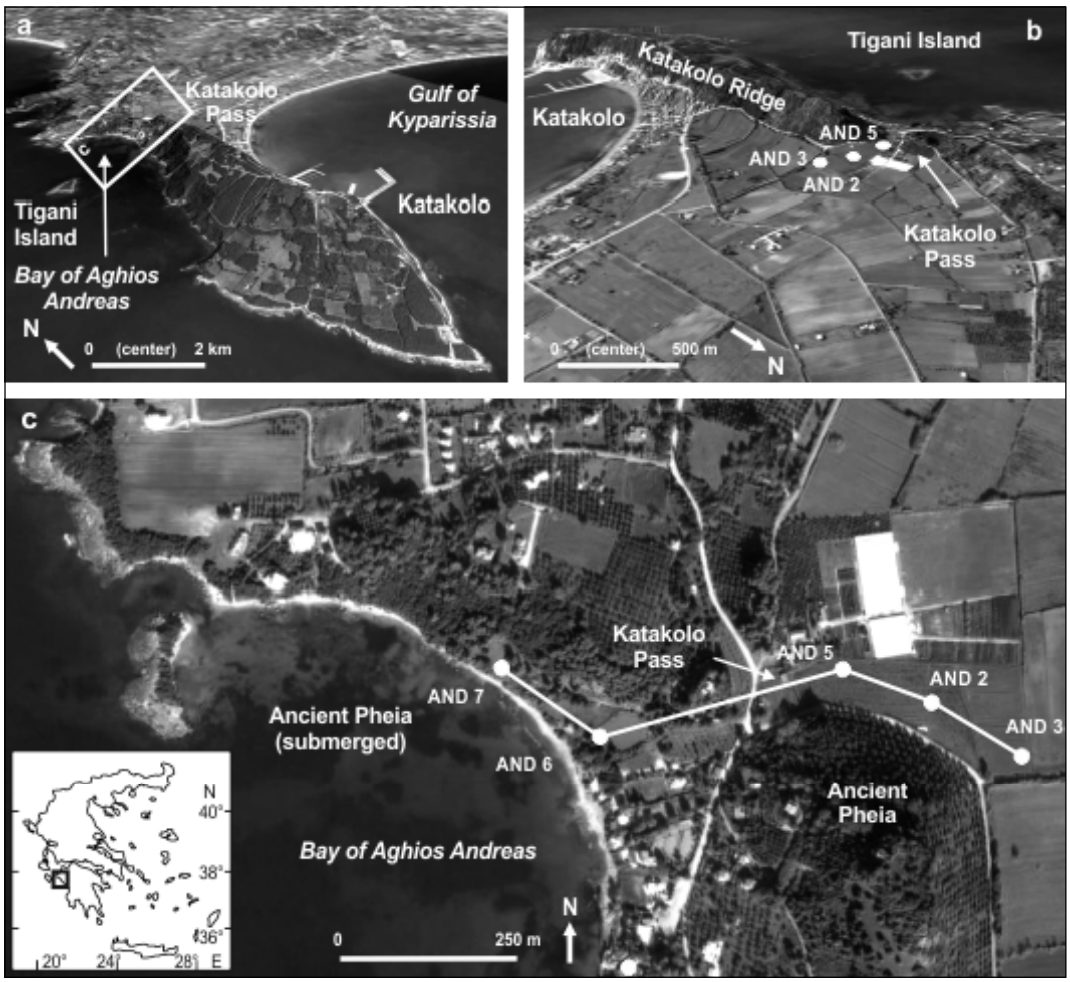

et al. 2004, *Guidoboni* and *Comastri* 2005, *Papadopoulos* et al. 2007, NGDC 2011). Based on historic catalogues, recurrence intervals for tsunami events – independent of their magnitude – were found highest for western Greece lying between 8 and 11 years only (*Soloviev* et al. 2000, *Schielein* et al. 2007). Last major seismogenic tsunami impacts occurred in the Strait of Messina (Italy) in 1908, in the central Aegean near the Islands of Astypalaea and Amorgos (Greece) in 1956, in the Gulf of Corinth (Greece) in 1996, and at Izmit (Turkey) in 1999, altogether killing more than 100,000 people (*Altınok* et al. 2001, *Papadopoulos* and *Fokaefs* 2005, *Billi* et al. 2008, *Okal* et al. 2009). The major tsunamigenic source is the Hellenic Trench, some 1200 km long and almost 5000 m deep, along which the Eurasian Plate is overriding the African Plate by a rate of up to 50 mm/a (*McClusky* et al. 2000). Subduction dynamics are responsible for numerous shallow earthquakes along the trench it-

Fig. 1 Topographic overview of the Bay of Aghios Andreas and the environs of ancient Pheia (Elis, western Peloponnese). *(a)* Bird's eye view to the ENE towards Cape Katakolo at the southern end of the Katakolo Promontory. The promontory is bounded by N-S trending tectonic faults. *(b)* Bird's eye view of the Katakolo and Aghios Ioannis coastal plains lying to the east of the Katakolo Promontory with coring sites AND 2, 3 and 5. *(c)* Detail photo map of the Katakolo Pass at the northern end of the Katakolo Promontory with the Katakolo Pass vibracore transect. The vibracore transect consists of cores AND 2, 3, 5, 6 and 7. The Bay of Aghios Andreas opens towards the west and conceals the submerged remains of ancient Pheia, one of the harbours of Olympia. See white rectangle in *Fig. 1a* for location of detail map section shown in *Fig. 1c*. Maps based on Google Earth images (2003)
Topographischer Überblick über die Bucht von Aghios Andreas und die Umgebung des antiken Pheia (Elis, Westpeloponnes). (a) Blick aus der Vogelperspektive nach Ost-Nordost in Richtung Kap Katakolo am südlichen Ende des gleichnamigen Bergsporns. Letzterer wird durch N-S streichende tektonische Störungen begrenzt. (b) Blick aus der Vogelperspektive auf die Küstenebenen von Katakolo und Aghios Ioannis östlich des Bergsporns von Katakolo mit den Bohrpunkten AND 2, 3 und 5. (c) Detailkarte des Passes von Katakolo am nördlichen Ende des Bergsporns mit dem passüberquerenden Bohrprofiltransekt aus den Bohrungen AND 2, 3, 5, 6 und 7. Die Bucht von Aghios Andreas öffnet sich nach Westen und verbirgt die unter Wasser befindlichen Reste des antiken Pheia, eines der Häfen von Olympia. Das weiße Rechteck in Fig. 1a beschreibt die Lage der Detailkarte von Fig. 1c. Kartengrundlage: Google Earth (2003)

self and associated fault systems (*Papazachos* and *Dimitriu* 1991).

During the past decades, especially after the tsunami shock of December 26, 2004 in south-east Asia, tsunami research has been strongly intensified. Research on (pre-)historic tsunami events may be considered as most suitable geoscientific measure to assess the present and future tsunami hazard of an area. In Greece, (palaeo-)tsunami deposits were found in the Aegean (*Pirazzoli* et al. 1999, *McCoy* and *Heiken* 2000, *Gaki-Papanastassiou* et al. 2001, *Pavlopoulos* et al. 2010), on Crete (*Scheffers* and *Scheffers* 2007, *Bruins* et al. 2008), on the southern Peloponnese (*Scheffers* et al. 2008), at the Gulf of Corinth (*Kontopoulos* and *Avramidis* 2003, *Alvarez-Zarikian* et al. 2008), on Lefkada Island and in coastal Akarnania (*Vött* et al. 2006, 2008, 2009a). Modelling (pre-)historic tsunami events has significantly contributed to our understanding of tsunami hydraulics, wave propagation and the dimensions of tsunami landfalls, in some cases it even initiated the detection and identification of new geoscientific traces. For the tsunamis that were associated to the Santorini eruption in the 17th century BC and the earthquake in western Crete in 365 AD, for example, modelling results (*Yokoyama* 1978, *Shaw* et al. 2008) are highly consistent with field evidence; far-distance teletsunamigenic deposits of these events were found on the Israeli coast (*Goodman-Tchernov* et al. 2009) and in northwestern Greece (*Vött* et al. 2009b), respectively.

Ancient Pheia is located in the Bay of Aghios Andreas (Elis, western Peloponnese) and was already subject to previous studies. *Kraft* et al. (2005) focused on neotectonics and coastal changes around Pheia, and *Fouache* and *Dalongeville* (1998a, 1998b, 2003, 2004) used the well-known beachrock sequences to reconstruct the local sea level history. Recent revision and geomorphological investigation of the Aghios Andreas beachrock, however, have brought to light that the beachrock cannot be considered as lithified beach deposits accumulated by littoral processes but represents the

post-depositionally cemented section of a Holocene tsunamite (*Vött* and *May* 2009, *Vött* et al. 2010). Based on these results, the main objectives of the studies presented in this paper are: (i) to search for geomorphological and sedimentological evidence of a tsunami impact along a vibracore transect from Pheia beach across Katakolo Pass, (ii) to use XRF analyses of sediment samples for tracing tsunamis, (iii) to establish an event-geochronostratigraphic framework, and (iv) to reconstruct the general tsunami flow dynamics and evaluate the overall significance of tsunami impacts for coastal evolution.

2. Physiogeographic Setting and Archaeological Background

Ancient Pheia is located on the western flank of the Katakolo Promontory, an almost 4 km long, N-S trending ridge extending into the Gulf of Kyparissia (*Fig. 1a*). The promontory is mainly built up of Neogene marl which is prone to landslides and, especially in the south, locally covered by Pleistocene marine deposits (IGMR 1980). The Katakolo Ridge, reaching up to 80 m above present mean sea level (m a.s.l.), separates the Bay of Aghios Andreas in the west from the Bay of Katakolo in the east. The first is a predominantly rocky shore with numerous smaller indentations characterised by cliffs, rock debris and beachrock, the second is a uniform sandy beach followed by a low-lying back beach zone that was artificially drained during the 1960s. The Katakolo Promontory is connected to the Peloponnese mainland via the narrow Katakolo Pass, only 30 m wide, with elevations of 18-20 m a.s.l. (*Figs. 1b* and *1c*; *Leake* 1830). The ridge is bound to parallel, N-S running fault systems, whereas the pass is associated to WSW-ENE trending secondary faults of minor dimension (IGMR 1980, *Kraft* et al. 2005). Towards both sides of Katakolo Pass, the slopes are of an alluvial-fan type; however, there is neither an alluvial system nor a torrential stream existing in the vicinity of the Katakolo Promontory. The small, ramp-like Tigani Island is located approximately 1 km to the southwest of Katakolo Pass offshore in the midst of the Bay of Aghios Andreas (*Fig. 1a*). Water depth in the bay does not exceed 5 m.

The archaeological remains of Pheia are widely spread around the Bay of Aghios Andreas. Remains of an ancient fortification system, called Pontikokastro, still exist on the southern flank above Katakolo Pass at approximately 60 m a.s.l. (*Leake* 1830). Oldest artifacts from the wider Katakolo area are from the Palaeolithic period (*McDonald* and *Hope Simpson* 1964). *Yalouris* (1957, 1960) found submerged traces of buildings and sherds from the 7th century BC to the Roman epoch in the Bay of Aghios Andreas. Onshore and further inland, trial excavations gave light to buildings and ceramics from every period from Early Helladic to Medieval times; on the Katakolo Promontory, a Cycladic-type marble figurine dating to the Early Bronze Age was found (*Hood* 1959/1960, *McDonald* and *Hope Simpson* 1964). From Tigani Island, tombs and buildings of Roman age are reported (*Hood* 1959/1960). Building material and ceramic fragments were also found incorporated into the Aghios Andreas beachrock, the youngest dating to the Byzantine epoch (*Yalouris* 1957, 1960, *Fouache* and *Dalongeville* 1998a, *Kraft* et al. 2005).

It is widely accepted that the remains near Aghios Andreas belong to ancient Pheia, one of the harbours of Olympia (*Strabo* 8, 2, 13, see *Groskurd* 1831) located some 28 km to the ESE of Katakolo Pass. Pheia is said to have been destroyed and sunk underwater during an earthquake in the 6th century AD (*Kraft* et al. 2005). For this time period, *Guidoboni* et al. (1994: 331ff.) list two major earthquakes that occurred in western Greece, one in 521 AD and another in 551 AD. The 551 AD earthquake is reported to have been related to a strong seismic sea wave which

brought destruction to many coastal cities on the Peloponnese and the Greek mainland (*Guidoboni* et al. 1994: 331ff.). *Meyer* (1979) suggests that the famous Temple of Zeus at Olympia collapsed during one of these seismic events.

3. Methods

Seven vibracores were drilled along a transect from the Bay of Aghios Andreas across Katakolo Pass towards the lowlands of the Bay of Katakolo. In this paper, original data from five vibracores are presented. Vibracoring was accomplished using a handheld engine-driven coring device (type Atlas Copco mk1) and core diameters of 6 and 5 cm. The maximum recovery depth was reached for core AND 5 with 15.50 m below ground surface (m b.s.). Vibracores were cleaned and photographed in the field and subsequently described using sedimentological and pedological methods (Ad-hoc-Arbeitsgruppe Boden 2005). Most important parameters were grain size and texture, colour, fossil content and pedogenic features. Marine macrofaunal remains were used for facies determination (*Lindner* 1999, *Poppe* and *Goto* 1991, 2000). Sediment samples were extracted from each major stratigraphic unit for geochemical analyses in the laboratory. Main geochemical parameters were electrical conductivity, pH-value (both measured in a suspension out of 15 g air-dried material and 75 ml distilled water), loss on ignition (measured by heating in the muffle furnace to 550°C), and carbonate content ($CaCO_3$, measured by means of the Scheibler method; *Schlichting* et al. 1995, *Barsch* et al. 2000).

XRF (x-ray fluorescence) analyses of sediment samples were accomplished using a handheld Thermo instrument, type Niton Xl3t 900S GOLDD. Measurements were carried out in the laboratory with original material using the SOIL software modus of the instrument. Each sample was continuously measured for 30 seconds using three different filters yielding mean relative concentrations per measured element. For standardisation and elimination of potential influences of grain size and moisture content, calculated elemental ratios were preferably used for interpretation. In total, around 30 elements were measured with a vertical resolution between several centimetres to decimetres per core depending on relevant changes in the stratigraphic record. XRF analyses by means of modern portable systems produce analytical results of high accuracy consistent with standard or specific calibrations, with results from traditional laboratory XRF systems, and with elemental concentrations measured in acidic solutions. This is documented by numerous studies on sediments, soils, artifacts and other materials (*Laohaudomchock* et al. 2010, *Pantazis* 2010, *Weindorf* et al. 2010, *Zhu* and *Weindorf* 2010).

Geochronological information was obtained by means of radiocarbon dating of plant remains and biogenetically produced carbonate as well as by archaeological age estimation of diagnostic sherds found embedded in vibracore sediments. Position and elevation of vibracoring sites and outstanding topographical elements were measured using a DGPS (type Topcon) with a horizontal and vertical accuracy < 1 cm.

4. Tsunami Signatures in the Environs of Pheia

Vött and *May* (2009) and *Vött* et al. (2010) conducted geomorphological and sedimentological investigations on beachrock outcrops along the beach in the Bay of Aghios Andreas (*Fig. 1c*). Key results of these studies are summarised in the following paragraph complemented by new observations of mega-clasts dislocated inland by high-energy impact.

4.1 The Aghios Andreas beachrock

In the southern part of the Bay of Aghios Andreas (*Fig. 1c*), the Aghios Andreas beachrock extends

vertically from several decimetres below present sea level (b.s.l.) some tens of metres offshore up to approximately 1.50 m above the present mean sea level (a.s.l.) where it disappears under a colluvial cover. In the central and northern parts of the bay, the beachrock reaches up to approximately 2.50 m a.s.l., resulting in a total thickness of up to 3 m (*Photo 1*). In the littoral zone, the beachrock is strongly eroded and scoured and lies partly embedded into recent littoral sand. Close to the chapel of Aghios Andreas, the beachrock can be subdivided into three different stratigraphic units (A, B and C). The lowermost unit (A) overlies Neogene marls on top of a clear erosional unconformity. It is a coarse-grained, badly-sorted conglomerate with pieces of gravel up to 15 cm in diameter including clasts of older Quaternary deposits. The second unit (B) is a thick stratum of medium to fine sand with local intercalations of coarse sand and fine gravel, abundant marine shell debris and ceramic frag-

Photo 1 (a) View of the northern and central parts of the Bay of Aghios Andreas with Katakolo Pass and remains of the fortification system of ancient Pheia (central middle ground). View direction is towards the SE. Inset photo shows a view from above Katakolo Pass towards the NW. Coring sites AND 6 and 7 are marked by white dots. *(b)* Outcrop of the Aghios Andreas beachrock in the central bay. The well-laminated mid-section of the beachrock sequence incorporates numerous large rip-up clasts, rocks from the littoral zone and man-made ashlars. The ashlar to the immediate right of the blue sunbed still has an angular shape and the original white plaster. Inset photo shows a beachrock outcrop from the southern part of the bay including numerous marine shell and ceramic fragments and signs of cross bedding. The Aghios Andreas beachrock is not a lithified *in situ* beach deposit but a post-depositionally cemented tsunamite (*Vött* and *May* 2009, *Vött* et al. 2010). See white rectangle in *Photo 1a* for location of detail *Photo 1b*. Photos taken by *A. Vött*, 2008, 2009 *Ansicht der nördlichen und zentralen Abschnitte der Bucht von Aghios Andreas mit dem Pass von Katakolo und Resten der Befestigungsanlage des antiken Pheia (Bildmitte). Die Blickrichtung ist gen SE. Das eingefügte Bild zeigt den Blick von einer Stelle südlich oberhalb des Passes von Katakolo gen NW. Die Bohrpunkte AND 6 und 7 sind durch weiße Punkte markiert. (b) Ausbiss des Beachrocks von Aghios Andreas in der zentralen Bucht. Der deutlich laminierte mittlere Abschnitt des Beachrocks enthält zahlreiche große Erosionsklasten aus anstehendem Gestein, Blöcke aus dem Festgesteinslitoral und menschgemachte Quader. Der Quader unmittelbar rechts der blauen Sonnenliege zeigt eckige Kanten und weißen Originalputz. Das eingefügte Detailphoto beschreibt einen Beachrock-Ausbiss im südlichen Buchtabschnitt. Der Beachrock enthält zahlreiche Muschel-, Schnecken- und Keramikbruchstücke und ist örtlich durch Kreuzschichtung gekennzeichnet. Der Beachrock von Aghios Andreas stellt keine lithifizierte in-situ-Strandablagerung dar, sondern einen post-sedimentär zementierten Tsunamiten (Vött und May 2009, Vött et al. 2010a). Das weiße Rechteck in Photo 1a bezeichnet die Lage des in Photo 1b abgebildeten Ausschnitts. Photos aufgenommen von A. Vött, 2008, 2009*

.

ments. Several fining-upward sequences as well as distinct lamination can be clearly discerned. In some places, this unit is covered by a mixed layer (C) of sand and gravel with abundant ceramic fragments, partly imbricated, and other terrigenous material. The set of sedimentary and geomorphological features encountered for the Aghios Andreas beachrock is clearly consistent with those characteristics that were found typical of subrecent and recent tsunami deposits all over the world (*Sato* et al. 1995, *Shi* et al. 1995, *Hindson* and *Andrade* 1999, *Fujiwara* et al. 2000, *Gelfenbaum* and *Jaffe* 2003, *Paris* et al. 2007).

It is especially the mid-section (B) of the Aghios Andreas beachrock that shows additional sedimentological characteristics which cannot be explained by littoral dynamics (*Vött* et al. 2010). In the central part of the bay, at elevations around 1-1.5 m a.s.l., we found (i) man-made ashlars incorporated into the sandy matrix, up to 50 x 30 x 20 cm^3 large, with angular edges and partly with remains of the original plaster, (ii) allochthonous stones and blocks, up to 50 cm in diameter, with encrustations of vermetids and other marine organisms and signs of bio-erosion associated to littoral zone dynamics, (iii) load casts underneath heavy ashlars and stones, (iv) convolute bedding structures, and (v) sharply edged ceramic fragments embedded in well-sorted, cross-bedded or laminated, multiply fining upward sandy sequences (*Photo 1*). Furthermore, sherds dating from the Mycenaean to the Roman period were found in near-coast shallow waters during previous archaeological studies without showing a stratigraphic order (*Kraft* et al. 2005, see Section 2).

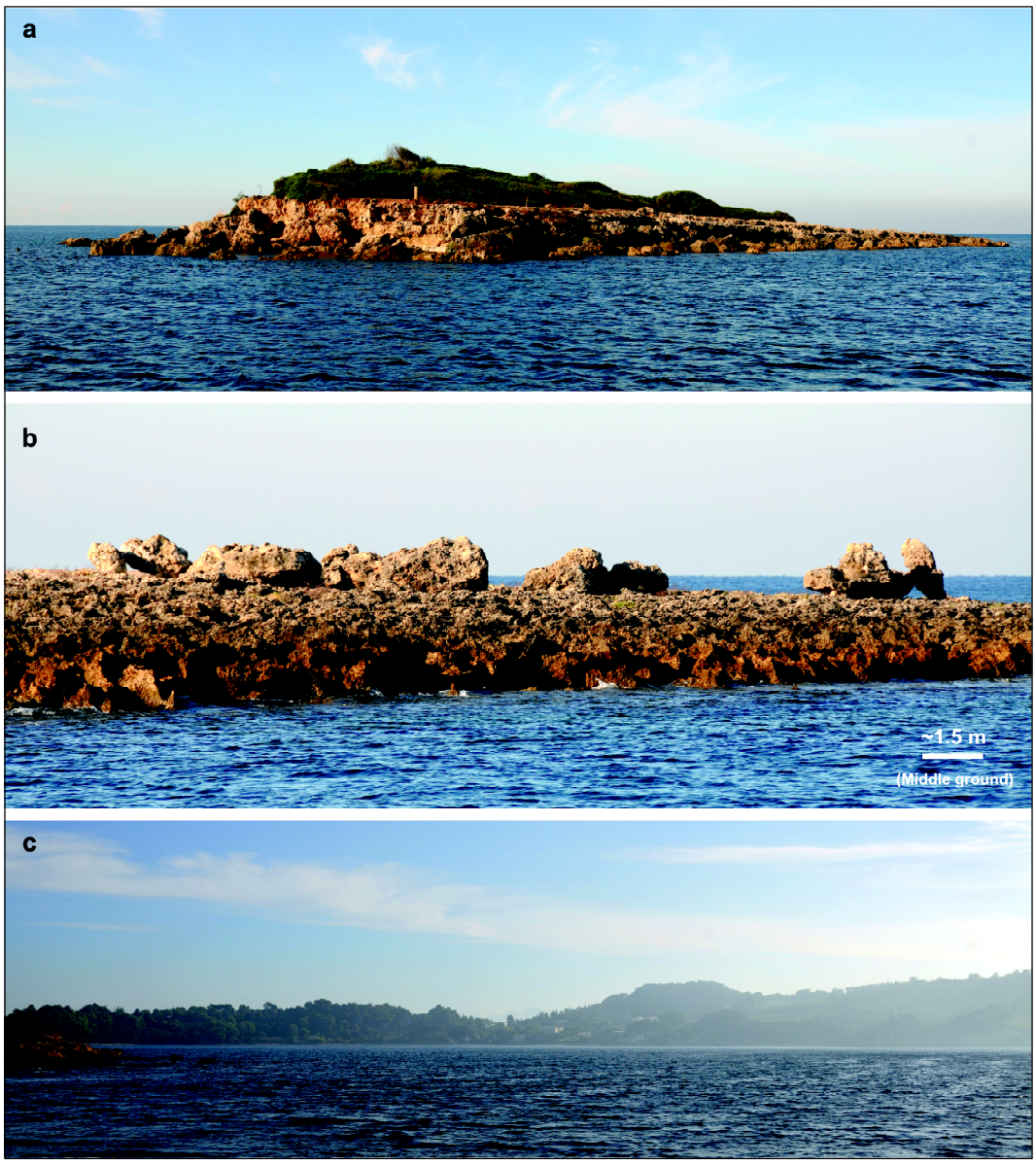

These field data document that sedimentation dynamics of the beachrock material was of a quick and high-energetic nature, related to an abrupt event coming from the seaside, and associated to the intense reworking of cultural and terrigenous deposits most probably originating from the harbour facilities of Pheia which, today, are lying submerged in the Bay of Aghios Andreas (*Fig. 1c*). Sharply edged ceramic fragments which are embedded in the

Photo 2 (a) Tigani Island in the Bay of Aghios Andreas. View towards the SW. Note the accumulation of large blocks below the cliff in a leeward position sheltered from storm wave action. *(b)* High-energy dislocated blocks from the littoral zone in the western part of Tigani Island. *(c)* View from Tigani Island towards the NE into the inner Bay of Aghios Andreas and Katakolo Pass (central middle ground, 18-20 m a.s.l.). During the mid- and late Holocene, the bay was hit by several strong tsunami events from a western direction. Tsunami waters repeatedly affected Tigani Island and, by channelling effects, overflowed Katakolo Pass. Photos taken by *A. Vött*, 2009 / *(a) Die Insel Tigani in der Bucht von Aghios Andreas, Blick nach SW. Besonders auffällig ist die Anhäufung von großen Blöcken unterhalb des Kliffs in leewärtiger, sturmwellengeschützter Lage. (b) Durch Hochenergieeinfluss dislozierte Blöcke aus Material des Festgesteinslitorals im westlichen Bereich der Insel Tigani. (c) Blick von der Insel Tigani nach NE in die zentrale Bucht von Aghios Andreas und den Pass von Katakolo (Bildmitte, 18-20 m ü. M.). Im mittleren und späten Holozän wurde die Bucht von mehreren starken Tsunami-Ereignissen aus westlicher Richtung erfasst. Wiederholt trafen die Tsunami-Wassermassen die Insel Tigani und überströmten den Pass von Katakolo aufgrund örtlicher Kanalisierungseffekte. Photos aufgenommen von A. Vött, 2009*

sandy deposits document abrupt, sudden and high-energy destruction of pottery untypical of normal littoral processes which only produce well rounded and abraded material. Partial cementation of the allochthonous high-energy deposits took place after deposition by pedogenic decalcification at the top, percolation of hydrocarbonate-saturated waters and secondary carbonate precipitation in lower sections of the high-energy deposit (*Vött* et al. 2010). Sedimentological characteristics of the beachrock material do clearly speak against long-lasting grinding, rounding and sorting processes as they are typical of the littoral zone.

Based on these observations, *Vött* and *May* (2009) and *Vött* et al. (2010) concluded that the Aghios Andreas beachrock is considered a cemented tsunamite which reflects three different phases of tsunamigenic influence, namely an initial phase of high-energy related erosion and unsorted deposition (unit A) during turbulent landfall and runup, an intermediate phase of well-sorting, lamination and fining-upward of sandy material (unit B) during inundation, and a final phase of mixed and unsorted deposition of marine and terrigenous material (unit C) during backflow. Load casting and convolute bedding are best explained by weight-induced gravity flows in water-saturated deposits shortly after deposition (*Füchtbauer* 1988), most probably in between different inundation impulses.

4.2 Dislocated blocks on Tigani Island

Tigani Island, lying approximately 1 km offshore in the Bay of Aghios Andreas (*Figs. 1a* and *1b*, *Photo 2c*), has a flat ramp-like relief reaching from present sea level in the west up to approximately 2.5 m a.s.l. in the east (*Photo 2a*). In its western part, numerous mega-blocks were found lying up to 1.5 m a.s.l. and 20-40 m distant from the coast. The mega-clasts are partly imbricated, partly lying in unstable constellations that reflect a high-energy impulse (*Photo 2b*). The estimated maximum size of the blocks is 2-4 m^3. As evidenced by (palaeo-)rock pools facing towards the ground or partly tilted from their original horizontal position, the blocks were torn out in the former littoral zone, lifted upon the ramp and transported inland. Dislocated mega-clasts were also found at the western flank of the Katakolo Promontory near Cape Katakolo. Dislocation of mega-blocks may

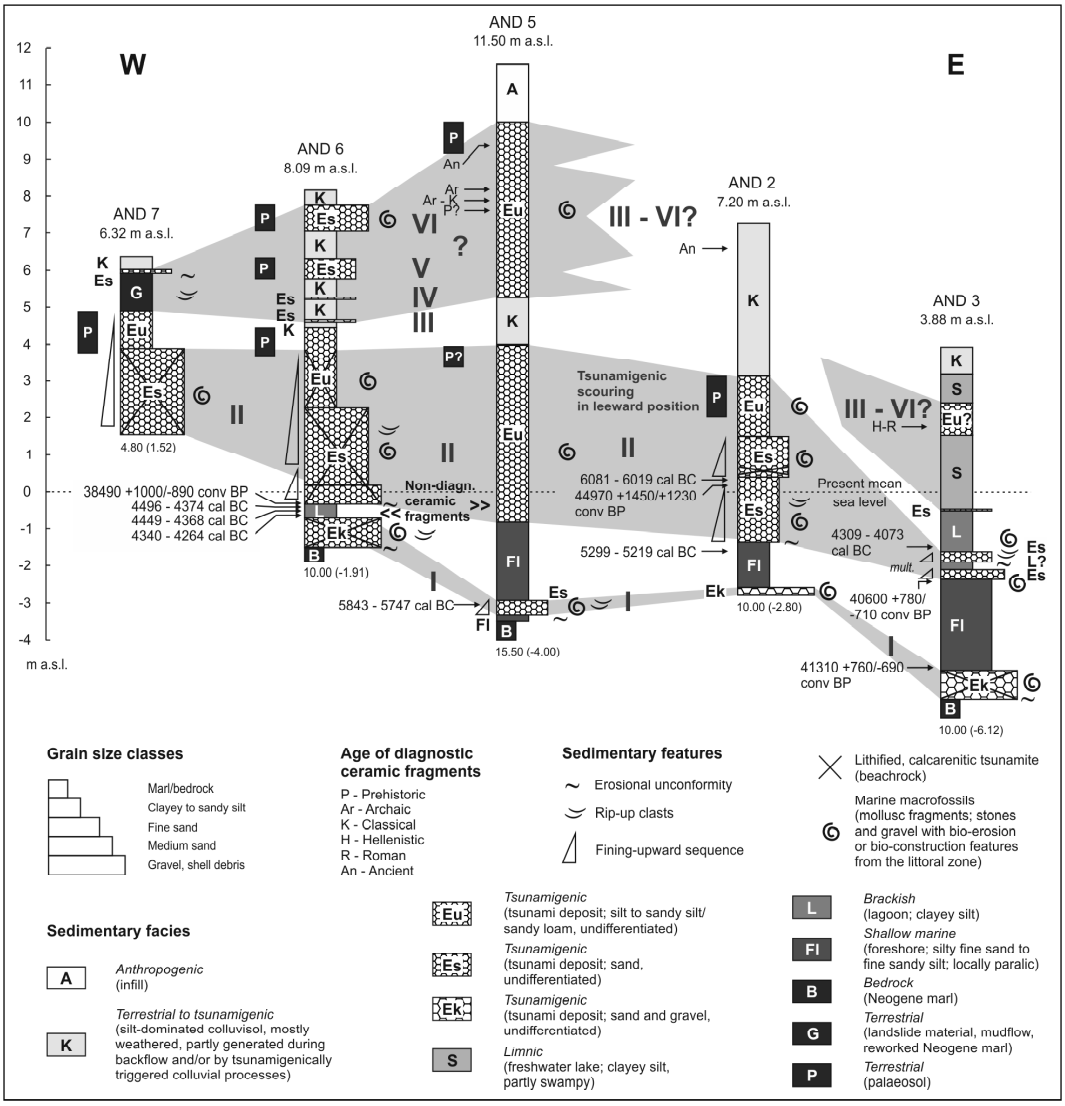

Fig. 2 Stratigraphies, facies distribution and geochronostratigraphy along the Katakolo Pass vibracore transect. For locations of vibracoring sites, see *Fig. 1*. For details on radiocarbon ages see *Table 1*. *Stratigraphien, Faziesverteilung und Geochronostratigraphie entlang des Bohrprofiltransektes über den Pass von Katakolo. Die Lage der einzelnen Bohrpunkte ist in Fig. 1 verzeichnet. Nähere Angaben zu den Radiokohlenstoff-Altern sind Tabelle 1 zu entnehmen.*

be due to single- or multi-phase transportation and is therefore difficult to interpret and to date. From a geomorphological point of view, however, massive rock debris and clast accumulations found on Tigani Island along a 2.5 m high distinct cliff in leeward position well sheltered from storm influence do not fit to the present geomorphodynamic situation and

cannot be explained by the principles of uniformitarianism (*Photo 2a*). Thus, the overall setting indicates complete inundation of Tigani Island by high-energy wave events and event-related block dislocation, leeward erosion and debris accumulation.

5. Event-Stratigraphic Record in Near-Coast Geological Archives

5.1 Vibracore transect across Katakolo Pass

Vibracores in the environs of ancient Pheia were drilled along a W-E running transect across Katakolo Pass lying at 18-20 m a.s.l. (*Figs. 1b* and *1c*). Stratigraphic details and facies distribution patterns are illustrated in *Figure 2*.

Vibracore AND 6 represents the key core for the western part of the transect. It was drilled at 8.09 m a.s.l. some 40 m distant from the present shore in a distal cliff top position behind a 30 m wide vegetation belt consisting of big trees and shrubs (*Photo 1*). At the base of AND 6, we encountered bluish-grey Neogene marl. On top of a distinct erosional unconformity, the marl is covered by a first sequence of beachrock of yellowish to light brown coarse sand and gravel including marine shell fragments and pieces of well rounded pebbles. This basal beachrock is subsequently overlain by brownish-grey clayey to silty deposits of a quiescent limnic freshwater environment, 37 cm thick, including plant remains and several non-diagnostic ceramic fragments. This layer is topped by another sharp disconformity and a more than 4 m thick unit of cemented light brown coarse sand with gravel, medium to fine sand and finally silt, showing at least two fining-upward sequences and containing marine macrofossil remains. Towards the top, the beachrock material turned dark brown in colour and disintegrated which reflects that stable conditions existed for a certain time period after the sediment was deposited and formed an *in situ* palaeosol. The upper section of core AND 6 is made up of alternating autochthonous colluvial and allochthonous marine deposits, the latter dominated by medium and fine brown sand and partly including marine shell debris. The colluvial material is made out of fine sandy, clayey silt, is light brown in colour and locally includes ceramic fragments and charcoal. *Ex situ* marine sandy deposits were found up to 7.69 m a.s.l.

Vibracore AND 7 was drilled at the western foot of a hill, more than 40 m high, of Neogene marl rising to the north of Katakolo Pass. In general, its stratigraphy is similar to the one found for core AND 6. However, we encountered a thick unit of unweathered Neogene bluish grey marl on top of the brownish beachrock and associated allochthonous deposits. This setting clearly documents gravity-induced landsliding processes towards the coast after the beachrock material was deposited. Landslides are characteristic geomorphological features of the regional, clay-dominated marly Neogene bedrock (IGMR 1980).

Vibracore AND 5 was drilled some 150 m to the east of Katakolo Pass at 11.50 m a.s.l. The grey Neogene bedrock is covered by shallow marine sediments out of grey fine and medium sand including laminae of organic matter (*Fig. 2*). A sharp erosional contact marks the boundary towards a subsequent shell debris layer, followed by fine to medium sand including rip-up clasts of Neogene bedrock, up to 10 cm large, and beachrock-type sandstone fragments. This unit is overlain by *in situ* shallow marine littoral deposits out of silty fine sand indicating that the original sedimentary environment had recovered after temporary disruption. Mid- and up-core sections of core AND 5 are characterised by two homogeneous and thick layers of sandy to silty deposits with marine shell debris separated by a reddish dark brown colluvisol out of predominantly silty material (*Fig. 2*). Each of the thick sandy to silty layers shows, in its uppermost part, evidence of soil formation such as a slightly

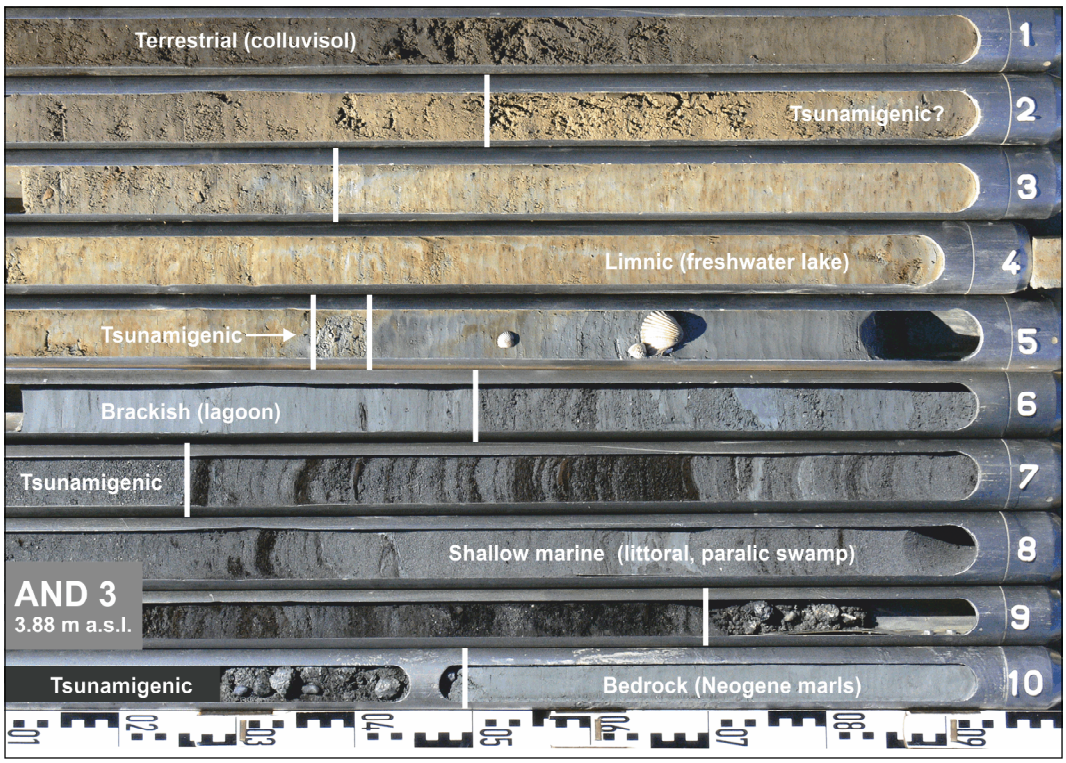

Fig. 3 Photo and simplified facies profile of sediment core AND 3 drilled in a leeward position in relation to Katakolo Pass, at a distance of roughly 650 m from Pheia beach. Photo taken by *T. Willershäuser*, 2009
Photo und vereinfachte Fasziesabfolge des Sedimentkerns AND 3, der in rund 650 m Entfernung vom heutigen Strand bei Pheia in leewärtiger Lage zum Pass von Katakolo erbohrt wurde. Photo aufgenommen von T. Willershäuser, 2009

higher content of clay, a strongly reduced content of calcium carbonate by weathering and a darker colour. Allochthonous shell fragments at site AND 5 were encountered up to 9 m a.s.l. Abundant non-diagnostic ceramic fragments were found in a stratigraphic position similar to core AND 6; further up-core, sherds from prehistoric (?) to Roman times were encountered.

Coring site AND 3 is located some 400 m towards the ESE of Katakolo Pass in a distal fan-type topographical situation at 3.88 m a.s.l. ground surface. We found an erosional contact in the bluish grey Neogene bedrock covered by partly cemented grey sandy gravel including many marine shell fragments (*Fig. 3*). Subsequently, a paralic swamp developed and persisted over a long time period as documented by blackish brown peat. Afterwards, alternating layers of grey fine sand and organic material were deposited in an intermediate paralic to littoral environment. Another sharp erosional unconformity marks an abrupt change towards predominantly medium grey sand showing several fining-upward sequences and including rip-up clasts out of Neogene marl and abundant marine shell debris. The allochthonous marine sand is covered by light grey lagoonal and later by brown to

grey limnic mud, both representing low-energy quiescent environments; another distinct layer of whitish grey fine to medium sand marks the immediate boundary between these two stratigraphic units. Further up-core, we found a slightly sandy intercalation in between brown to grey limnic deposits, the latter being finally covered by a dark brown colluvisol including small ceramic fragments. The stratigraphy of the neighbouring core AND 2 is very similar. However, the AND 2 mid-core marine sands appear in the form of a distinct beachrock-type calcarenite (*Vött* et al. 2010) and, towards the top, where the beachrock is strongly disintegrated, by a well-developed reddish-brown palaeosol.

In a summary view, allochthonous deposits along the Katakolo Pass transect were found up to 10 m a.s.l. and 400 m (AND 5) to 650 m (AND 3) distant from the present shore (*Figs. 1* and *2*). These *ex situ* deposits are clearly associated to high-energy impact features such as erosional unconformities, rip-up clasts, fining-upward sequences and landslides. Taking into consideration that local autochthonous sedimentary conditions are those of colluvial (AND 7, 6, 5, 2) or limnic (AND 3) depositional environments, and that there is no evidence of either past or present torrential activity in the environs of Katakolo Pass, these *ex situ* marine deposits reflect repeated high-energy wave impact on the Bay of Aghios Andreas. Along with the geomorphological and sedimentological findings from the Aghios Andreas beachrock, our results further document repeated flooding of Katakolo Pass triggered by high-energy waves. Based on strong stratigraphic correlations, we were able to differentiate between six different generations of such high-energy deposits (generations I to VI, *Fig. 2*). The maximum number of allochthonous high-energy deposits was found at coring site AND 6. The transect also reveals a general trend of thinning and fining inland of the deposits dependent on the local pre-existing topography (*Fig. 2*).

5.2 Ca-Fe ratios

XRF analyses were accomplished for sediment samples from different stratigraphic units encountered in vibracores; their vertical resolution is therefore dependent on the number of samples taken per core. By XRF analyses, the concentrations of approximately 30 elements were measured. We calculated Ca-Fe ratios for each core in order to obtain a dimensionless relative tool for evaluating differences in the measured values for the stratigraphic record. Vertical profiles of Ca-Fe ratios are displayed in *Figure 4* with regard to the topographic setting. Measured concentrations (in %) for Fe were maximum 3.75 ± 0.05 (AND 3) and minimum 0.33 ± 0.02 (AND 6), for Ca maximum 48.16 ± 0.54 (AND 7) and minimum 0.86 ± 0.04 (AND 5). Average Fe concentrations per core (in %) range between 1.39 ± 0.04 (AND 2) and 1.98 ± 0.05 (AND 3), average Ca concentrations per core (in %) between 8.25 ± 0.19 (AND 5) and 22.53 ± 0.31 (AND 7).

Ca and Fe reach their maximum concentrations in diametrically opposed sedimentary environments. The input of Ca into the coastal system is mainly due to the biogenic production of calcium carbonate under saltwater-dominated marine conditions, for example by molluscs, foraminifers and ostracods, and Ca is also imported as dissolved component in the water. On the contrary, Fe is a major product of weathering and soil formation and thus relatively enriched in terrestrial environments. The Ca-Fe ratio thus enhances the differences between the geochemical and mineralogical fingerprints of marine and terrestrial environments. Marine sediments are characterised by high Ca-Fe ratios; terrestrial deposits by low Ca-Fe ratios.

Tsunamis in the Mediterranean, unlike storms or other processes in the littoral zone, are capable to transport marine sediments far inland and produce marine interferences in terrestrial, semi-terrestrial or limnic stratigraphies. Ca-Fe ratios

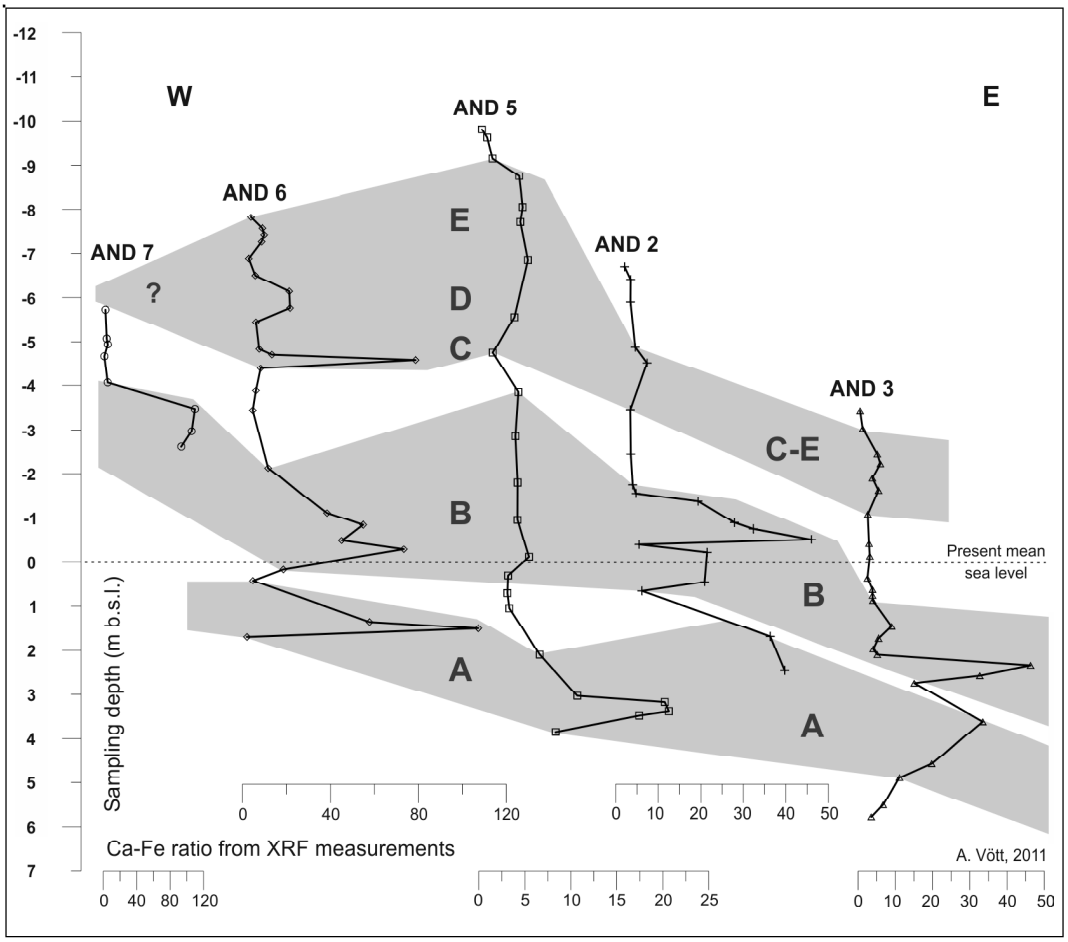

Fig. 4 Ca-Fe ratios for vibracores along the Katakolo Pass transect derived from XRF measurements. The group of graphs shows several distinct interferences (A to E) that can be traced across the pass, lying at 18-20 m a.s.l., and up to several hundreds of metres inland (AND 2 and 3).
Ca-Fe-Verhältniszahlen für Bohrkerne entlang des Transektes über den Pass von Katakolo. Die Daten basieren auf XRF-Messungen. Die Kurvenverläufe veranschaulichen mehrere deutliche Störungen (A bis E), die über den Pass hinweg mehrere Hundert Meter landeinwärts verfolgt werden können (AND 2 und 3). Der Pass selbst liegt auf 18-20 m ü. M.

may therefore serve as reliable tsunami tracers. Due to the clearly semi-humid regional climate of the western Peloponnese where annual precipitation reaches amounts of 800-1000 mm (*Lienau* 1989), predominantly during the cold winter season (November to April), and produces strong downward percolation, the formation of carbonate crusts by ascending pore water within terrestrial deposits as known from semi-arid and arid climate zones (*Kleber* 2002) can be neglected. However, in case of long enduring subaerial weathering of Ca-rich terrigenous and/or marine deposits onshore, the original Ca-Fe signal will be locally weakened by decalcification and

downward percolation of dissolved calcium carbonate, and locally increased in lower sedimentary layers by recrystallisation. In such a case, the Ca-Fe ratio represents a mixed signal; as recrystallisation preferentially affects coarse-grained stratigraphic units that induce a strongly and abruptly reduced pore volume towards the underlying material, allochthonous coarse-grained high-energy deposits are expected to become even more accentuated by this process. Considering the overall sedimentological frame and pedogenic processes, the Ca-Fe ratio was successfully used for tracing tsunami deposits 1 km inland in the Palairos coastal plain in northwestern Greece (*Vött* et al. 2011).

Figure 4 illustrates that cores AND 6, 5, 2 and 3 show a distinct sequence of several Ca-Fe peaks that are separated by intervals of low Ca-Fe values. Taking into consideration that cores AND 6, 5 and 3 reached the local Neogene bedrock, the different vertical Ca-Fe profiles can be easily correlated. In *Figure 4*, different phases of interference of the local autochthonous sedimentary environment are labelled with capital letters A to E from the base towards the top. Interference A is clearly identifiable as the oldest interference in cores AND 6, 5 and 3. Interference B is characterised by a neat double peak in cores AND 6, 2 and 3, whereas in core AND 5 there is only a weak signal. The latter may occur when, by decalcification and pedogenic processes, the macroscopic fossil fingerprint of an *ex situ* layer is already weak or has completely disappeared (see *Fig. 2*). Interferences C to E are most clearly visible in core AND 6. Deposits of tsunami generation IV encountered in core AND 6 (*Fig. 2*) are not reflected in *Figure 4* because no sample was taken from this stratigraphic unit for XRF measurements.

Compared to the AND core stratigraphies, Ca-Fe ratio interferences A to E (*Fig. 4*) perfectly correspond to high-energy wave impacts as documented in *Figure 2*. Moreover, our results show that Ca-Fe ratios can be used to establish a reliable relative event-geochronology based on exceptional and characteristic attributes of the vertical Ca-Fe profiles such as the double peak appearance of interference B.

5.3 Dating approaches

In this paper, we present 11 radiocarbon dates used for establishing a local event-geochronological framework. Calibrated radiocarbon dates are listed in *Table 1*. Where possible, we preferred plant material instead of marine shells for dating in order to eliminate a potential marine reservoir effect. The dimension of fluctuations of the marine reservoir effect in space (sedimentary environments) and time (stratigraphic position) are still unknown. In case of sample AND 6/21+ M (Kia 39787) the given radiocarbon age of 38,490 +1,000/-890 BP lies beyond existing calibration datasets so that the correction of the marine reservoir is not feasible. All other samples except AND 6/21+ PR (Kia 39784) show $\delta^{13}C$ values typical of C3 plants so that a reservoir effect can be excluded. This is also true for the seaweed sample AND 6/22+ PR (Kia 39786, $\delta^{13}C = -4.98 \pm 0.15$) reflecting a shallow-water shallow marine environment. The low $\delta^{13}C$ value of sample AND 6/21+ PR (Kia 39784, $\delta^{13}C = -15.50 \pm 0.30$), however, indicates that the dated material was polluted by C4 plant detritus or that it comes from an aquatic plant. The latter case would imply that a marine reservoir effect has to be taken into account. Cross-checking with more reliable dates of the neighbouring samples AND 6/21+ PR2 and AND 6/22+ PR (Kia 39785 and Kia 39786, *Table 1*) allows to suggest that the potential reservoir effect of sample AND 6/21+ PR (Kia 39784) is, however, close to nil. Radiocarbon dating was accomplished by the Leibniz Laboratory for Radiometric Dating and Isotope Research, Christian-Albrechts-Universität zu Kiel (Kia) using the high-accuracy ^{14}C AMS technique.

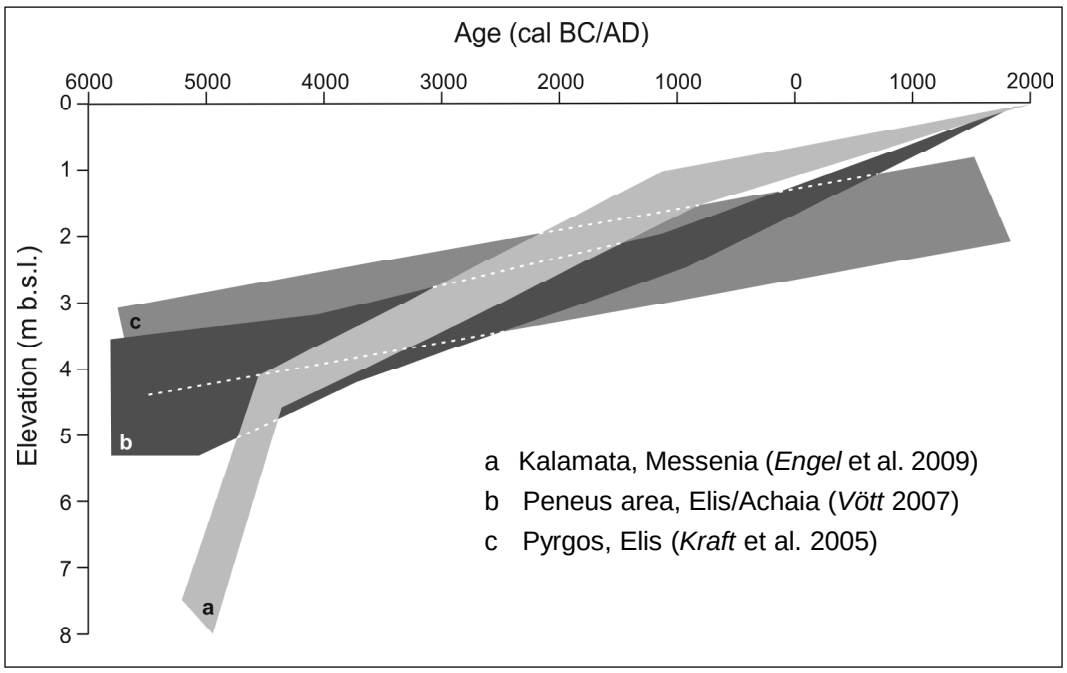

Fig. 5 Relative sea level bands reconstructed for the western and southwestern Peloponnese by different authors based on radiocarbon dated sedimentological sea level indicators encountered in vibracores. It can be clearly seen that during the Holocene the sea level has never been higher than at present. *Verlaufsbänder des relativen Meeresspiegels, wie sie von unterschiedlichen Autoren auf der Grundlage von radiokohlenstoffdatierten sedimentologischen Meeresspiegelindikatoren aus Bohrkernen für die westliche und südwestliche Peloponnes vorliegen. Es ist deutlich erkennbar, dass der relative Meeresspiegel im Verlauf des Holozäns nie höher lag als heute.*

As the radiocarbon dating method cannot be used to date the time of sediment deposition itself but rather yields the time of death of embedded organic samples, radiocarbon dates used for the geomorphological reconstruction of landscape or sedimentary changes have always to be considered as mere approximations. With regard to palaeo-tsunami investigations, the most promising approach is to date samples from autochthonous sedimentary units both overlying and underlying the tsunamite (sandwich dating approach) because tsunamites as such may contain abundant reworked organic material and would thus produce mere maximum ages. Finally, the radiocarbon based *termini ante* and *post quem* for tsunami events are all the more reliable the lesser the differences in depth between sample and tsunamite; however, in case of tsunamigenic erosion of underlying geological units a hiatus of unknown dimension has to be taken into account. For all these reasons and in order to not pretend an accuracy which cannot be guaranteed, we decided to use 1σ intervals for calibrated radiocarbon ages rounded to centuries for the final geochronological interpretation.

Moreover, diagnostic ceramic fragments encountered in the cores were used for archaeological

age determination. Calibrated radiocarbon dates and archaeological age estimates are shown in *Figure 2* within their stratigraphic context.

6. Discussion

6.1 Relative sea level evolution

Based on the results of *Yalouris* (1957, 1960) and their own investigations, *Fouache* and *Dalongeville* (1998a, 1998b, 2003, 2004) drew up a complex scenario of the late Holocene coastal and relative sea level evolution in the environs of Pheia. Their basic assumptions were (i) that the archaeological remains of ancient Pheia were found down to 5 m water depth between Tigani Island and the present beach, and (ii) that the beachrock – interpreted as lithified littoral deposit – reaches up to 1.50 m a.s.l. and includes potsherds from Roman to Byzantine times. Their scenario suggests gradual subsidence of ancient Pheia between Classical and Byzantine times down to 6.5 m b.s.l. inducing a sandy littoral system to move inland in the form of a transgression. The upper part of the littoral sands was cemented to beachrock due to a subsequent uplift of 1.5 m; according to the authors, the uplift, however, was also of a slow and gradual nature. Using the Aghios Andreas beachrock as sea level indicator, *Fouache* and *Dalongeville* (1998a, 1998b, 2003, 2004) thus assume a yo-yo type fluctuation of the relative sea level comprising a gradual sea level rise by 6.5 m and a subsequent gradual sea level fall by 1.5 m between the mid-first millennium BC and Byzantine to post-Byzantine times. Abrupt crustal movements along the N-S trending Katakolo Promontory faults were negated by the authors because the beachrock appears as a continuous sequence without breaks from below present sea level up to 1.5 m a.s.l.

Fouache and *Dalongeville* (1998a, 1998b, 2003, 2004) did not consider the sedimentary characteristics of the beachrock but concentrated on its overall appearance and elevation. *Vött* and *May* (2009) and *Vött* et al. (2010) showed by detailed geomorphological and sedimentological studies that the Aghios Andreas beachrock must not be regarded as lithified beach deposits but rather as the cemented parts of a tsunamite (Section 4; for correlation of the Aghios Andreas beachrock with high-energy wave deposits encountered in vibracores, see Section 6.3). Hence, it is not acceptable to use the beachrock as relative sea level indicator. By *Vött* et al. (2010 and in this study), beachrock deposits at Pheia were actually found to reach up to 2.5 m a.s.l. in the central part of the bay (Section 4) which means another 1 m higher than observed by *Fouache* and *Dalongeville* (1998a, 1998b). This would, however, result in a total vertical movement and sea level change of 7.5 m (submergence) + 2.5 m (uplift) = 10 m within 1000 or so years, yielding an average rate of 10 mm/a.

Continuous, long-term DGPS monitoring of the crustal evolution revealed an overall 2-4 mm/a subsidence of the Ionian Islands with respect to the northwestern Greek mainland (*Hollenstein* et al. 2008a). One of the DGPS stations used is located at Keri on the southern coast of Zakynthos Island only some 42 km to the WSW of the Bay of Aghios Andreas. By similar DGPS measurements, *Hollenstein* et al. (2008b) found evidence of co-seismic vertical displacement within the range of 1-2 decimeters for the Strophades Island lying some 50 km to the SSW of Cape Katakolo during the Mw 6.6 Strophades earthquake in 1997. Moreover, intense relative sea level studies were conducted around Pyrgos, in Elis and Achaia, and in Messenia by *Kraft* et al. (2005), *Vött* (2007) and *Engel* et al. (2010) at a distance of 11 km, 20 km and 100 km of ancient Pheia, respectively. By these studies, relative sea level curves were established based on reliable sedimentological indicators encountered in vibracores and dated by

the radiocarbon method. *Figure 5* shows the reconstructed band width for the relative sea level for each study area. There are no essential differences in relative sea level evolution; the western and southwestern Peloponnese shows a more or less constant sea level rise of 0.5-0.7 mm/a. Considerable relative tectonic subsidence of several metres is only revealed for Messenia for the time before 4500 cal BC (*Engel* et al. 2009).

Based on these data, we summarise that a vertical yo-yo movement of the sea level in the range of altogether 8 to 10 m within 1000 years (*Fouache* and *Dalongeville* 1998a, 1998b, see above) is not realistic. As there is no reason to suggest that the relative sea level evolution around Pheia differs considerably from the general trend reconstructed for the immediate environs, we assume a gradual relative sea level rise of maximum 1.5-3 m for the last 3000 or so years (maximum 0.5-1.0 mm/a, *Fig. 5*). Moreover, like in many other regions in the eastern Mediterranean, the relative sea level in the western Peloponnese has never been higher than today (*Fig. 5*).

Vött and *May* (2009) and *Vött* et al. (2010) showed that the Aghios Andreas beachrock at Pheia represents a tsunamite and must not be used as a sea level indicator. Concerning the use of underwater archaeological remains as sea level indicator, it has to be clarified whether they represent *in situ* or rather dislocated findings; in the latter case, they, too, should not be used for relative sea level reconstruction. Finally, coseismic displacements could be at least partly responsible for the submergence of ancient Pheia and cannot be excluded for the area. Additionally, we know that they may go hand in hand with tsunami landfall and the inland deposition of tsunami deposits; for example, coseismic subsidence occurred parallel to the Chile 1960, the Izmit 1999 and the Indian Ocean 2004 tsunamis (*Altınok* et al. 2001, *Meltzner* et al. 2006, *Searle* 2006, *Nelson* et al. 2009, *Reinhardt* et al. 2010).

6.2 Storm versus tsunami impact

The western Peloponnese is characterised by prevailing winds and thus wind-generated waves from western and northwestern directions (Medatlas Group 2004). Buoy measurements in the open Ionian Sea between Italy and Greece revealed maximum wave heights of up to 4-7 m (*De Martini* et al. 2010, see also *Soukissian* et al. 2007). For the inner Ionian Sea off the western Peloponnese, the mean significant wave height during the winter season is lower than 1.2 m and the probability that significant wave heights exceed 4 m in near-coast areas is almost nil (Medatlas Group 2004, *Cavaleri* 2005). Offshore the northwestern Peloponnese, significant wave periods and heights of deep water waves of < 6 sec and < 3 m, respectively, were observed (*Poulos* and *Chronis* 2001). Based on gauge records, *Tsimplis* and *Shaw* (2010) further showed that seasonal sea level extremes occur during the autumn and winter months and are less than 40 cm which is the lowest value in the eastern Mediterranean. It may thus be concluded that the overall wave regime and the susceptibility towards storm events in the studied area is only moderate to weak.

Against the background of 20-75 strong tropical-like storms, so-called Medicanes, that occur in the Mediterranean per century (*Pytaroulis* et al. 2000, *Fita* et al. 2007), exceptional storm events are frequent and thus expected to leave more or less regular low- to mid-energy signatures in local sedimentary environments. *Sabatier* et al. (2008), for example, found that storm-borne sand layers, only a few centimetres thick, are flushed into a coastal lagoon in southern France every 50-100 years. In contrast, the high-energy deposits described in this paper reflect a high to extreme magnitude and low frequency event pattern.

There are thus strong arguments for interpreting high-energy deposits encountered at Pheia beach and along the Katakolo Pass vibracore transect as tsunami and not as storm deposits.

(i) Historic accounts and catalogues report on repeated tsunami landfall along the coasts of the western Peloponnese (Section 2). In contrast, there is no written source documenting exceptionally strong winter storms and the related destruction of coastal infrastructure.

(ii) The present beach at Aghios Andreas has a width of 10 m only, extended to maximum 20 m during storms (*Fig. 1, Photo 1*). Like in other parts of the Gulf of Kyparissia, there is neither subrecent to recent geomorphological nor sedimentological evidence that winter storms affect the outer-littoral zone and reach further inland.

(iii) High-energy deposits were found up to 10 m a.s.l. and 650 m inland (*Fig. 2*). They were transported across and deposited beyond Katakolo Pass at 18-20 m a.s.l. Highest storm-borne wave heights reported from the open Ionian Sea are 6-7 m and have peak periods shorter than 15 sec (*Scicchitano* et al. 2007, *Bertotti* and *Cavaleri* 2009). Moving onshore, wave heights and the mobilised volume of water are not sufficient to overtop Katakolo Pass or even to transport and deposit *ex situ* marine sediments, up to 4 m thick (AND 2, *Fig. 2*), to a leeward position. The spatial dimensions reflected by the allochthonous deposits around Pheia are too large to be caused by storm wave activity. This is all the more true because the local relative sea level during the Holocene has never been higher than at present (Section 6.1).

(iv) Taking into consideration the geographical position and dimension of the high-energy deposits encountered around Pheia (*Figs. 1* and *2*), sedimentary characteristics such as erosional unconformities, incorporated rip-up clasts from the underlying units, multiple fining-upward sequences – as found typical for tsunamites of numerous subrecent to recent events (Section 4) – speak for a tsunamigenic rather than a storm-borne formation.

(v) Sedimentary and textural characteristics of the Aghios Andreas beachrock comprise extensive load casting and convolute bedding structures (*Photo 1*). These features indicate slow gravity-driven flow dynamics within a thick water-saturated viscous sedimentary matrix shortly after sediment deposition. They are untypical of littoral and storm deposits but well-known for turbidites (*Füchtbauer* 1988) and tsunamites (*Bhattacharya* and *Bandyopadhyay* 1998, *Rossetti* et al. 2000, *Plaziat* et al. 2006).

6.3 Local tsunami geochronostratigraphy

Radiocarbon dating yielded four ages between 38,000-45,000 conv BP (*Tab. 1*) lying close to the radiocarbon detection limit. We cross-checked these dates with other ages obtained for the corresponding vibracores (*Fig. 2*). Samples AND 6/21+ M (Kia 39787) and AND 2/15 PR (Kia 39778) are clearly identifiable as reworked material of pre-Holocene age. As for samples AND 3/18+ PR (Kia 39781) and AND 3/22+ PR (Kia 39780), the strong stratigraphic correlations between cores AND 2 and AND 3 document that they, too, are the result of reworking and incorporation of older sediments into the Holocene sequence. In the light of our sedimentological and stratigraphic results (*Fig. 2*, Section 5), the yielded high percentage of samples (36 %) with pre-Holocene ages reflects that a strong high-energy impact affected the pre-existing coastal morphology and led to intense erosion and dislocation of older deposits.

Table 1 Radiocarbon dates of samples from vibracores drilled along the Katakolo Pass transect in the environs of ancient Pheia (Elis). Note: b.s. – below ground surface; b.s.l. – below sea level; 1σ max; min cal BP/BC (AD) – calibrated ages, 1σ-range; ";" – semicolon is used in cases where there are several possible age intervals due to multiple intersections with the calibration curve; Lab. No. – laboratory number, Leibniz Laboratory for Radiometric Dating and Isotope Research, Christian-Albrechts-Universität zu Kiel (Kia); [a] δ^{13}C-value shows incorporation of C4 plants or aquatic plant material and indicates a potential reservoir effect; [b] δ^{13}C-value indicates purely atmospheric C3 photosynthesis without contamination by old carbon. Calibration based on Calib 6.0 software (*Reimer* et al. 2009) / *Radiokohlenstoffalter von Proben aus Bohrkernen entlang des Transekts über den Pass von Katakolo in der Umgebung des antiken Pheia (Elis). Beachte: b.s. – unter Geländeoberfläche; b.s.l. – unter heutigem Meeresspiegel; 1σ max; min cal BP/BC (AD) – kalibriertes Alter, 1σ-Intervall; ";" – das Semikolon bedeutet, dass es aufgrund mehrerer Überschneidungsbereiche mit der Kalibrierungskurve mehrere mögliche Altersintervalle gibt; Lab. No. – Labor-Nummer, Leibniz-Labor für Altersbestimmung und Isotopenforschung, Christian-Albrechts-Universität zu Kiel (Kia);* [a] *der δ^{13}C-Wert zeigt die Beteiligung von C4-Pflanzen oder Wasserpflanzen an und deutet auf einen potenziellen Reservoireffekt hin;* [b] *der δ^{13}C-Wert dokumentiert ausschließlich atmosphärische C3-Photosynthese ohne Kontaminierung durch alten Kohlenstoff. Die Kalibrierung erfolgte mittels Calib 6.0-Software (Reimer et al. 2009).*

Sample Name	Depth (m b.s.)	Depth (m b.s.l.)	Sample Description	Lab. No. (Kia)	δ^{13}C (ppm)	^{14}C Age (BP)	1σ max; min (cal BP)	1σ max; min (cal BC)
AND 2/14+ PR	6.85	- 0.35	Plant remains, indeterminable	39777	-27.94 ± 0.51[b]	7205 ± 35	8030 - 7968	6081 - 6019
AND 2/15 PR	6.98	- 0.22	Wood fragment	39778	-23.28 ± 0.21[b]	44970 +1450/-1230	-	-
AND 2/17+ PR	8.74	1.54	Wood fragment	39779	-29.49 ± 0.14[b]	6265 ± 35	7248; 7168	5299; 5219
AND 3/14+ PR	5.41	1.53	Plant remains, indeterminable	39782	-30.60 ± 0.13[b]	5350 ± 30	6258; 6022	4309; 4073
AND 3/18+ PR	6.28	2.40	Peat, wood fragment	39781	-30.08 ± 0.13[b]	40600 +780/-710	-	-
AND 3/22+ PR	8.65	4.77	Wood fragment	39780	-26.69 ± 0.11[b]	41310 +760/-690	-	-
AND 5/19 PR	14.54	3.04	Wood fragment	39783	-27.48 ± 0.15[b]	6390 +40/-35	7792 - 7696	5843 - 5747
AND 6/21+ M	8.43	0.34	Bivalve fragment, undetermined	39787	-0.21 ± 0.21	38490 +1000/-890	-	-
AND 6/21+ PR	8.56	0.47	Plant fragments, indeterminable	39784	-15.50 ± 0.30[a]	5625 ± 30	6445; 6323	4496; 4374
AND 6/21+ PR2	8.55	0.46	Plant fragments, indeterminable	39785	-24.40 ± 0.22[b]	5580 ± 35	6398; 6317	4449; 4368
AND 6/22+ PR	8.62	0.53	Seaweed remains	39786	-24.98 ± 0.15[b]	5445 ± 30	6289; 6213	4340; 4264

Concerning tsunami generation I, we found an age of 5843-5747 cal BC in core AND 5 (Kia 39783); as this sample was taken from the tsunamigenic unit itself, reworking effects cannot be excluded so that the age has to be considered as *terminus ad quem*, at best, or as *terminus post quem* for the corresponding event (*Fig. 2*). Tsunami deposits dated to the same time interval at the beginning of the 6th millennium BC were recently identified at several sites in coastal Akarnania lying some 130 km to the WNW of the study area (*Vött* et al. 2009a, 2009b, 2011).

Radiocarbon ages obtained for cores AND 6, 2 and 3 provide a quasi-sandwich dating constellation for tsunami event II (*Fig. 2*). For core AND 6, there are three consistent ages from the underlying unit of tsunamite II (AND 6/22+ PR, AND 6/21+ PR2, AND 6/21+ PR, Kia 39786-39784, *Tab. 1*), the time interval 4500-4300 cal BC representing a neat *terminus post quem* for the corresponding event. A sample from the base of lagoonal deposits covering tsunamite II in core AND 3 yielded an additional *terminus ante quem* of 4309-4073 cal BC (AND 3/14+ PR, Kia 39782) for tsunami generation II which was rounded to 4300-4100 cal BC. This results in a time interval between 4500-4300 cal BC and 4300-4100 cal BC during which tsunami event II must have occurred, that means around 4300 ± 200 cal BC.

Ages obtained for core AND 2 do not contradict this conclusion. The lower sample AND 2/17+ PR dated to 5299-5219 cal BC (Kia 39779) is considered a *terminus post quem* for event II. In the light of the sharp erosional contact found in the hosting shallow marine deposits (*Fig. 2*), a hiatus of several hundreds of years seems to be realistic. Regarding stratigraphic correlations, the upper sample AND 2/14+ PR (Kia 39777) from inside the tsunamite – yielding a maximum age of 6081-6019 cal BC – has to be considered as reworked. In a wider regional context, strong sedimentological and geochronological evidence of a tsunami event around 4400 cal BC was found in cores from the Palairos coastal plain in Akarnania, northwestern Greece (*Vött* et al. 2011). This implies the possibility of another supra-regional tsunami record in western Greece for the mid-Holocene.

Regarding tsunami generations III to VI, age estimates for diagnostic ceramic fragments found in sediment cores prove that the area was affected by strong tsunami landfall in historic times. Youngest fragments were dated to the ancient period, that is between Classical and Roman times (*Fig. 2*). More precise dating is based on correlations with the Aghios Andreas beachrock outcrops along the beach.

Ashlars and ceramic fragments incorporated into the Aghios Andreas beachrock date to Roman to Byzantine times thus yielding a *terminus ad* or *post quem* for the corresponding tsunami event (*Vött* et al. 2010, Section 2). Compared to the overall geochronostratigraphic pattern obtained by vibracoring across Katakolo Pass (*Fig. 2*), the Aghios Andreas beachrock would thus correlate to event III, IV, V or VI; to clarify this question, we calculated the elevation of the Aghios Andreas beachrock to be expected at a distance of 40 m from the shore and compared it to the stratigraphy of key core AND 6. These calculations are based on an average seaward inclination of 7° found for the well laminated mid-section strata of the Aghios Andreas beachrock (*Fouache* and *Dalongeville* 1998a, *Vött* et al. 2010).

In the southern part of the bay, the uppermost visible part of the beachrock was found at an elevation of 1.50 m a.s.l., some 8 m distant from the waterfront. For a distance of 40 m from the coast – which corresponds to the inland position of coring site AND 6 – this results in a projected elevation of the beachrock of approximately 5.80 m a.s.l.

In the central part of the bay, in the direct prolongation of our vibracore transect towards the coast, the uppermost and the lowermost visi-

ble sections of the Aghios Andreas beachrock lie at elevations of 2.5 m a.s.l. and 1 m a.s.l., respectively, some 4 m inland. The projected elevation range of the tsunamite thus is 5.80-7.20 m a.s.l. at site AND 6.

Comparing these results with the stratigraphy of core AND 6 (*Fig. 2*), both scenarios strongly suggest that the Aghios Andreas beachrock outcrops along the beach, dating to Byzantine to post-Byzantine times, correspond to tsunamite generations V or VI which were encountered in core AND 6 at 5.72-6.26 m a.s.l. and 6.99-7.69 m a.s.l., respectively (*Fig. 2*). Consequently, by this projection, tsunamite V or VI can be dated indirectly to the Byzantine or post-Byzantine period, that means to the 4th century AD or younger times. Based on the facts that (i) cultural remains younger than the Byzantine epoch are neither incorporated into the Aghios Andreas beachrock nor in tsunamites V or VI, and (ii) a seismically generated tsunami occurred in 551 AD according to historic accounts (Section 2), we however assume that Pheia was finally destroyed by an earthquake and tsunami in 551 AD, most probably accompanied by sudden co-seismic subsidence (Section 6.1). Our data further show that the youngest beachrock generation found along the beach forms a wedge-like accretion to older tsunamigenic beachrock units with a strong thinning inland tendency.

In a regional event-geochronological context, sedimentary evidence of the oldest tsunamite generation at Pheia which was dated to the beginning of the 6th millennium BC is also known from several other coastal areas in continental northwestern Greece and the Ionian Islands (*Vött* et al. 2009a, 2009b, 2011). This may indicate tsunamigenic devastation, shifting of coastlines and massive dislocation of sediment within a large, eventually even supra-regional frame. Further, a tsunamite deposited in the 5th millennium BC, probably around 4400 cal BC, was detected in the Bay of Palairos-Pogonia which is located around 130 km towards the NNW right across the inner Ionian Sea (*Vött* et al. 2011). Based on the stratigraphic and geochronological consistency with tsunamite generation II at Pheia dated to 4300 ± 200 cal BC (this paper), it is hypothesised that a large event hit the entire region and led to considerable coastline changes. Moreover, Lake Voulkaria in NW Greece as well as onshore and offshore sediment archives in eastern Sicily revealed sediments most probably associated to the 365 AD tsunami (*Vött* et al. 2009b, *De Martini* et al. 2010, *Smedile* et al. 2011). This time window may also fit to young tsunami signals at Pheia dated to Byzantine to post-Byzantine times; however, written sources are in favour of the year 551 AD when a seismic sea wave is reported to have hit the area.

In a summary view, our geoscientific studies revealed multiple strong tsunami impact on the Bay of Aghios Andreas, some core stratigraphies consisting of up to 40-80 % of tsunamigenic deposits. The large number of small indentations, rocky islands, and large clasts of rock debris and the wide distribution of tsunamigenic beachrock indicate that the littoral dynamics typical of our days have not yet been able to recover and to re-establish a balanced coastal system since the last tsunami hit the area. The present coastal environment in the Bay of Aghios Andreas and its vicinity must be regarded as the result of ruinous tsunami impact (*Fig. 1*). Our results show that the overall significance of tsunamigenic destruction for the Holocene coastal evolution of the study area is far greater than gradual processes resulting in cliff erosion, longshore drift and coastal aggradation.

7. Conclusions

Detailed geomorphological, sedimentological, geochemical and geochronological investigations in the environs of ancient Pheia, Elis,

western Peloponnese, result in the following conclusions:

(i) The Aghios Andreas beachrock represents the post-depositionally cemented, calcarenitic part of a tsunamite of Byzantine to post-Byzantine age consisting of high-energy dislocated marine deposits. It therefore must not be used as sea level indicator. During the Holocene, the relative sea level at Pheia is suggested to have never been higher than at present.

(ii) The Katakolo Pass vibracore transect revealed that authochthonous sedimentary environments were repeatedly interfered by high-energy input of allochthonous marine sediments. Six different generations of tsunami impact (I to VI) were discerned.

(iii) Tsunami deposits were encountered up to 10 m a.s.l. and 650 m inland. By tsunami inundation, Katakolo Pass, at 18-20 m a.s.l., was repeatedly overflowed from west to east. Tsunami deposits reveal clear thinning inland tendencies. Ca-Fe ratios of tsunami deposits were used to trace and correlate tsunami signatures.

(iv) The oldest tsunami impact (I) probably occurred at the beginning of the 6th millennium BC. Thickest tsunami deposits were found for impact generation II representing the major tsunami shock for the site. It was sandwich-dated by the radiocarbon method to 4300 ± 200 cal BC. Younger generations of tsunami landfall (III to VI) mostly occurred in historic times. The Aghios Andreas beachrock outcrops along Pheia beach, dated to Byzantine to post-Byzantine times, correlate with generation V or VI and represent the final destruction of the ancient harbour of Olympia. Most probably, it was deposited in 551 AD when a seismic sea wave hit the site according to historic accounts.

Acknowledgements

We thank *E. Brunotte, C. Curdt, D. Hoffmeister, S.M. May* (Universität zu Köln) and *S. Ivy-Ochs* (Eidgenössische Technische Hochschule Zürich) for joint field survey and *K. Baika* (University of the Peloponnese, Kalamata) for discussion. Intense discussion and valuable support during field work by *G. Chatzi-Spiliopoulou* (7th Ephorate of Prehistoric and Classical Antiquities, Hellenic Ministry of Culture, Olympia), *H.-J. Gehrke* (Albert-Ludwigs-Universität Freiburg) and *R. Senff* (German Archaeological Institute, DAI, Athens) are gratefully acknowledged. We thank *M. Leopold* (Technische Universität München) and an anonymous reviewer for valuable comments that helped to improve the manuscript. Work permits were kindly issued by the Greek Institute of Geology and Mineral Exploration (IGME, Athens). Field and laboratory studies were conducted within the framework of the interdisciplinary project "Quaternary Tsunami Events in the Eastern Ionian Sea" funded by DFG (German Research Foundation, Bonn, VO 938/3-1).

8. References

Ad-hoc-Arbeitsgruppe Boden der Staatlichen Geologischen Dienste und der Bundesanstalt für Geowissenschaften und Rohstoffe 2005: Bodenkundliche Kartieranleitung. – 5. Auflage.– Stuttgart, Hannover

Altınok, Y., S. Tinti, B. Alpar, A.C. Yalçincer, Ş. Ersoy, E. Bortolucci and *A. Armigliato* 2001: The Tsunami of August 17, 1999 in Izmit Bay, Turkey. – Natural Hazards **24**: 133-146

Alvarez-Zarikian, C.A., S. Soter and *D. Katsonopoulou* 2008: Recurrent Submergence and Uplift in the Area of Ancient Helike, Gulf of Corinth, Greece: Microfaunal and Archaeological Evidence. – Journal of Coastal Research **24** (1A): 110-125

Barsch, H., K. Billwitz und *H.-R. Bork* (Hrsg.) 2000: Arbeitsmethoden in Physiogeographie und Geoökologie. – Gotha, Stuttgart

Bertotti, L. and *L. Cavaleri* 2009: Large and Small Scale Wave Forecast in the Mediterranean Sea. – Natural Hazards and Earth System Sciences **9**: 779-788. – Online available at: http://www.nat-hazards-earth-syst-sci.net/9/779/2009/nhess-9-779-2009.pdf, 16/02/2011

Bhattacharya, H.N. and *S. Bandyopadhyay* 1998: Seismites in a Proterozoic Tidal Succession, Singhbhum, Bihar, India. – Sedimentary Geology **119** (3): 239-252

Billi, A., R. Funiciello, L. Minelli, C. Faccenna, G. Neri, B. Orecchio and *D. Presti* 2008: On the Cause of the 1908 Messina Tsunami, Southern Italy. – Geophysical Research Letters **35**: L06301. – Online available at: http://www.andreabilli.com/2008_Billietal_GRL.pdf, 16/02/2011

Bruins, H.J., J.A. MacGillivray, C.E. Synolakis, C. Benjamini, J. Keller, H.J. Kisch, A. Klügel and *J. van der Plicht* 2008: Geoarchaeological Tsunami Deposits at Palaiokastro (Crete) and the Late Minoan IA Eruption of Santorini. – Journal of Archaeological Science **35** (1): 191-212

Cavaleri, L. 2005: The Wind and Wave Atlas of the Mediterranean Sea – The Calibration Phase. – Advances in Geosciences **2**: 255-257. – Online available at: http://www.adv-geosci.net/2/255/2005/adgeo-2-255-2005.pdf, 16/02/2011

De Martini, P.M., M.S. Barbano, A. Smedile, F. Gerardi, D. Pantosti, P. Del Carlo and *C. Pirrotta* 2010: A Unique 4000 Year Long Geological Record of Multiple Tsunami Inundations in the Augusta Bay (Eastern Sicily, Italy). – Marine Geology **276** (1-4): 42-57

Engel, M., M. Knipping, H. Brückner, M. Kiderlen and *J.C. Kraft* 2009: Reconstructing Middle to Late Holocene Palaeogeographies of the Lower Messenian Plain (Southwestern Peloponnese, Greece): Coastline Migration, Vegetation History, and Sea Level Change. – Palaeogeography, Palaeoclimatology, Palaeoecology **284** (3-4): 257-270

Fita, L., R. Romero, A. Luque, K. Emanuel and *C. Ramis* 2007: Analysis of the Environments of Seven Mediterranean Tropical-like Storms Using an Axisymmetric, Nonhydrostatic, Cloud Resolving Model. – Natural Hazards and Earth System Sciences **7**: 41-56. – Online available at : http://www.nat-hazards-earth-syst-sci.net/7/41/2007/nhess-7-41-2007.pdf, 17/02/2011

Fouache, E. and *R. Dalongeville* 1998a: Neotectonics in Historical Times: The Example of the Bay of Aghios Andreas (Ilia, Greece). – Zeitschrift für Geomorphologie **42** (3): 367-372

Fouache, E. et *R. Dalongeville* 1998b: De la nécessaire prise en compte des sédiments dans la connaissance des variations récentes de la ligne de rivage: exemples d'Aghios Andreas (Grèce) et de Guverdjine Kaya (Syrie). – Géomorphologie: Relief, Processus, Environnement **2**: 131-140. – Disponible en ligne à: http://www.persee.fr/web/revues/home/prescript/article/morfo_1266-5304_1998_num_4_2_950, 17/02/2011

Fouache, E. and *R. Dalongeville* 2003: Recent Relative Varations in the Shorelines: A Contrastive Approach of the Shores of Croatia and Southern Turkey. – In: *Fouache, E.* (ed.): The Mediterranean World: Environment and History. – IAG Working Group on Geo-Archaeology, Symposium Paris, Université de Paris-Sorbonne, 24-26 April 2002, Proceedings. – Paris: 467-478

Fouache, E. and *R. Dalongeville* 2004: Neotectonic Impact on Relative Sea-Level Fluctuations over the Past 6000 Years: Examples from Croatia, Greece and Southern Turkey. – In: CIESM (Commission Internationale pour l'Exploration Scientifique de la Mer Méditerranée): Human Records of Recent Geological Evolution in the Mediterranean Basin – Historical and Archaeological Evidence. – Workshop Santorini 22-25 October 2003. – CIESM Workshop Monographs **24**: 43-50

Füchtbauer, H. (Hrsg.) 1988: Sedimente und Sedimentgesteine. – Sediment-Petrologie **2**. – 4. Aufl. – Stuttgart

Fujiwara, O., F. Masuda, T. Sakai, T. Irizuki and *K. Fuse* 2000: Tsunami Deposits in Holocene Bay Mud in Southern Kanto Region, Pacific Coast of Central Japan. – Sedimentary Geology **135** (1-4): 219-230

Gaki-Papanastassiou, K., H. Maroukian, D. Papanastassiou, N. Palyvos and *F. Lemeille* 2001: Geomorphological Study in the Lokrian Coast of Northern Evoikos Gulf (Central Greece) and Evidence of Palaeoseismic Destructions. – Rapports du Commission Internationale pour l'Exploration Scientifique de la Mer Méditerranée (CIESM) **36**: 25. – Online available at : http://www.ciesm.org/online/archives/abstracts/index.htm, 18/02/2011

Gelfenbaum, G. and *B. Jaffe* 2003: Erosion and Sedimentation from the 17 July, 1998 Papua New Guinea Tsunami. – Pure and Applied Geophysics **160** (10-11): 1969-1999

Goodman-Tchernov, B.N., H.W. Dey, E.G. Reinhardt, F. McCoy and *Y. Mart* 2009: Tsunami

Waves Generated by the Santorini Eruption Reached Eastern Mediterranean Shores. – Geology **37** (10): 943–946

Groskurd, C.G. 1831: Strabos Erdbeschreibung in siebzehn Büchern, verdeutscht von Christoph Gottlieb Groskurd. – 4 Bände. – Wiederabdruck der Ausgabe von 1831-1834, 1988. – Hildesheim

Guidoboni, E., A. Comastri and *G. Traina* 1994: Catalogue of Ancient Earthquakes in the Mediterranean Area up to the 10th Century, Volume **1**. – Bologna

Guidoboni, E. and *A. Comastri* 2005: Catalogue of Earthquakes and Tsunamis in the Mediterranean Area from the 11th to the 15th Century, Volume **2**. – Bologna

Hindson, R.A. and *C. Andrade* 1999: Sedimentation and Hydrodynamic Processes Associated with the Tsunami Generated by the 1755 Lisbon Earthquake. – Quaternary International **56** (1): 27-38

Hollenstein, C., M.D. Müller, A. Geiger and *H.-G. Kahle* 2008a: Crustal Motion and Deformation in Greece from a Decade of GPS Measurements, 1993-2003. – Tectonophysics **449** (1-4): 17-40

Hollenstein, C., M.D. Müller, A. Geiger and *H.-G. Kahle* 2008b: GPS-Derived Coseismic Displacements Associated with the 2001 Skyros and 2003 Lefkada Earthquakes in Greece. – Bulletin of the Seismological Society of America **98** (1): 149-161. – Online available at: http://mahabghodss.net/NewBooks/www/web/digital/nashrieh/bssa/2008/Feb%202008,%20Vol.% 2098%20issue%201/10/10.pdf, 18/02/2011

Hood, M.S.F. 1959/1960: Archaeology in Greece, 1959. – Archaeological Reports **6**: 3-26

IGMR (Institute of Geological and Mining Research) 1980: Geological Map of Greece, 1:50,000, Pirgos Sheet (Mapped by *H. Streif*). – Athens

Kleber, A. 2002: Kalkanreicherungshorizont. – In: *Brunotte, E., H. Gebhardt, M. Meurer, P. Meusburger* und *J. Nipper* (Hrsg.): Lexikon der Geographie in vier Bänden, Band **2**. – Heidelberg, Berlin: 193

Kontopoulos, N. and *P. Avramidis* 2003: A Late Holocene Record of Environmental Changes from the Aliki Lagoon, Egion, North Peloponnesus, Greece. – Quaternary International **111**: 75-90

Kraft, J.C., G.R. Rapp, J.A. Gifford and *S.E. Aschenbrenner* 2005: Coastal Change and Archaeological Settings in Elis. – Hesperia **74** (1): 1-39. – Online available at: http://muse.jhu.edu/journals/hesperia/v074/74.1kraft.pdf, 24/02/2011

Laohaudomchok, W., J.M. Cavallari, S.C. Fang, X. Lin, R.F. Herrick, D.C. Christiani and *M.G. Weisskopf* 2010: Assessment of Occupational Exposure of Manganese and Other Metals in Welding Fumes by Portable X-ray Fluorescence Spectrometer. – Journal of Occupational and Environmental Hygiene **7** (8): 456-465

Leake, W.M. 1830: Travels in the Morea: with a Map and Plans. – Volume 1-3. – London

Lienau, C. 1989: Griechenland. Geographie eines Staates der europäischen Südperipherie. – Darmstadt

Lindner, G. 1999: Muscheln und Schnecken der Weltmeere: Aussehen, Vorkommen Systematik. – 5. Aufl. – München et al.

McClusky, S., S. Balassanian, A. Barka, C. Demir, S. Ergintav, I. Georgiev, O. Gurkan, M. Hamburger, K. Hurst, H. Kahle, K. Kastens, G. Kekelidze, R. King, V. Kotzev, O. Lenk, S. Mahmoud, A. Mishin, M. Nadariya, A. Ouzounis, D. Paradissis, Y. Peter, M. Prilepin, R. Reilinger, I. Sanli, H. Seeger, A. Tealeb, M.N. Toksoz and *G. Veis* 2000: Global Positioning System Constraints on Plate Kinematics and Dynamics in the Eastern Mediterranean and Caucasus. – Journal of Geophysical Research, Solid Earth **105** (B3): 5695-5719

McCoy, F.W. and *G. Heiken* 2000: Tsunami Generated by the Late Bronze Age Eruption of Thera (Santorini), Greece. – Pure Applied Geophysics **157** (6-8): 1227–1256

McDonald, W.A. and *R.Hope Simpson* 1964: Further Exploration in Southwestern Peloponnese: 1962-1963. – American Journal of Archaeology **68** (3): 229-245

Medatlas Group 2004: Wind and Wave Atlas of the Mediterranean Sea. – Paris, Athens

Meltzner, A.J., K. Sieh, M. Abrams, D.C. Agnew, K.W. Hudnut, J.-P. Avouac and *D.H. Natawidjaja* 2006: Uplift and Subsidence Associated with the Great Aceh-Andaman Earthquake 2004. – Journal of Geophysical Research, Solid Earth **111**(2): B02407

Meyer, E. 1979: Olympia. – In: *Ziegler, K.* und *W. Sontheimer* (Hrsg.): Der kleine Pauly: Lexikon der Antike auf der Grundlage von Pauly's Realency-

clopädie der classischen Altertumswissenschaft. Band **4**. – München: 279-284

National Geophysical Data Center (NGDC): NOAA/ WDC Historical Tsunami Database at NGDC. – Online available at: http://www.ngdc.noaa.gov/hazard/tsu_db.shtml, 07/02/2011

Nelson, A.R., K. Kashima and *L.-A. Bradley* 2009: Fragmentary Evidence of Great-Earthquake Subsidence during Holocene Emergence, Valdivia Estuary, South Central Chile. – Bulletin of the Seismological Society of America **99** (1): 71-86

Okal, E.A., C.E. Synolakis, B. Uslu, N. Kalligeris and *E. Voukouvalas* 2009: The 1956 Earthquake and Tsunami in Amorgos, Greece. – Geophysical Journal International **178** (3): 1533-1554

Pantazis, T., J. Pantazis, A. Huber and *R. Redus* 2010: The Historical Development of the Thermoelectrically Cooled X-Ray Detector and its Impact on the Portable and Hand-held XRF Industries. – X-Ray Spectrometry **39** (2): 90-97

Papadopoulos, G.A. and *A. Fokaefs* 2005: Strong Tsunamis in the Mediterranean Sea: A Re-Evaluation. – ISET Journal of Earthquake Technology **42** (4): 159-170. – Online available at: http:// home.iitk.ac.in/~vinaykg/Iset463.pdf, 22/02/2011

Papadopoulos, G.A., E. Daskalaki, A. Fokaefs and *N. Giraleas* 2007: Tsunami Hazards in the Eastern Mediterranean: Strong Earthquakes and Tsunamis in the East Hellenic Arc and Trench System. – Natural Hazards and Earth System Sciences **7** (1): 57-64. – Online available at: http://www.nat-hazards-earth-syst-sci.net/7/57/2007/nhess-7-57-2007.pdf, 22/02/2011

Papazachos, B.C. and *P.P. Dimitriu* 1991: Tsunamis in and Near Greece and Their Relation to the Earthquake Focal Mechanism. – Natural Hazards **4** (2-3): 161-170

Paris, R., F. Lavigne, P. Wassmer and *J. Sartohadi* 2007: Coastal Sedimentation Associated with the December 26, 2004 Tsunami in Lhok Nga, West Banda Aceh (Sumatra, Indonesia). – Marine Geology **238** (1-4): 93-106

Pavlopoulos, K., M. Triantaphyllou, P. Karkanas, K. Kouli, G. Syrides, K. Vouvalidis, N. Palyvos and *T. Tsourou* 2010: Palaeoenvironmental Evolution and Prehistoric Human Environment in the Embayment of Palamari (Skyros Island, Greece) during Middle-Late Holocene. – Quaternary International **216** (1-2): 41-53

Pirazzoli, P.A., S.C. Stiros, M. Arnold, J. Laborel and *F. Laborel-Deguen* 1999: Late Holocene Coseismic Vertical Displacements and Tsunami Deposits Near Kynos, Golf of Euboea, Central Greece. – Physics and Chemistry of the Earth, Part A: Solid Earth and Geodesy **24** (4): 361-367

Plaziat, J.-C., M. Aberkan and *J.-L. Reyss* 2006: New Late Pleistocene Seismites in a Shoreline Series Including Eolianites, North of Rabat (Morocco). – Bulletin de la Société Géologique de France **177** (6): 323-332

Poppe, G.T. and *Y. Goto* 1991: European Seashells. Volume I: Polyplacophora, Caudofoveata, Solenogastra, Gastropoda. – Wiesbaden

Poppe, G.T. and *Y. Goto* 2000: European Seashells. Volume II: Scaphopoda, Bivalvia, Cephalopoda. – Hackenheim

Poulos, S.E. and *G.T. Chronis* 2001: Coastline Changes in Relation to Longshore Sediment Transport and Human Impact along the Shoreline of Kato Achaia (NW Peloponnese, Greece). – Mediterranean Marine Science **2** (1): 5-13. – Online available at: http://www.medit-mar-sc.net/files/200812/17-11473105-13.pdf, 22/02/2011

Pytharoulis, I., G.C. Craig and *S.P. Ballard* 2000: The Hurricane-Like Mediterranean Cyclone of January 1995. – Meteorological Applications **7** (3): 261-279

Reimer, P.J., M.G.L. Baillie, E. Bard, A. Bayliss, J.W. Beck, P.G. Blackwell, C. Bronk Ramsey, C.E. Buck, G.S. Burr, R.L. Edwards, M. Friedrich, P.M. Grootes, T.P. Guilderson, I. Hajdas, T.J. Heaton, A.G. Hogg, K.A. Hughen, K.F. Kaiser, B. Kromer, F.G. McCormac, S.W. Manning, R.W. Reimer, D.A. Richards, J.R. Southon, S. Talamo, C.S.M. Turney, J. van der Plicht and *C.E. Weyhenmeyer* 2009: IntCal09 and Marine09 Radiocarbon Age Calibration Curves, 0-50,000 Years Cal BP. – Radiocarbon **51** (4): 1111-1150. – Online available at: http:// research commons.waikato.ac.nz/bitstream/10289/ 3622/1/ogg%20Intcal09%20and%20Marine09.pdf, 22/02/2011

Reinhardt, E.G., R.B. Nairn and *G. Lopez* 2010: Recovery Estimates for the Río Cruces after the May 1960 Chilean Earthquake. – Marine Geology **269** (1-2): 18-33

Rossetti, D.D.F., A.M. Góes, W. Truckenbrodt and *J. Anaisse* 2000: Tsunami-Induced Large-Scale Scour-

and-Fill Structures in Late Albian to Cenomanian Deposits of the Grajaú Basin, Northern Brazil. – Sedimentology **47** (2): 309-323

Sabatier, P., L. Dezileau, M. Condomines, L. Briqueu, C. Colin, F. Bouchette, M. Le Duff and *P. Blanchemanche* 2008: Reconstruction of Paleostorm Events in a Coastal Lagoon (Hérault, South of France). – Marine Geology **251** (3-4): 224-232

Sato, H., T. Shimamoto, A. Tsutsumi and *E. Kawamoto* 1995: Onshore Tsunami Deposits Caused by the 1993 Southwest Hokkaido and 1983 Japan Sea Earthquakes. – Pure and Applied Geophysics (PAGEOPH) **144** (3/4): 693-717

Scheffers, A. and *S. Scheffers* 2007: Tsunami Deposits on the Coastline of West Crete (Greece). – Earth and Planetary Science Letters **259** (3-4): 613-624

Scheffers, A., D. Kelletat, A. Vött, S.M. May and *S. Scheffers* 2008: Late Holocene Tsunami Traces on the Western and Southern Coastlines of the Peloponnesus (Greece). – Earth and Planetary Science Letters **269** (1-2): 271-279

Schielein, P., J. Zschau, H. Woith und *G. Schellmann* 2007: Tsunamigefährdung im Mittelmeer: Eine Analyse geomorphologischer und historischer Zeugnisse. – In: *Schellmann, G.* (Hrsg.): Bamberger physisch-geographische Studien 2002-2007. Teil 1: Holozäne Meeresspiegelveränderungen, ESR-Datierungen aragonitischer Muschelschalen, Paläotsunamis. – Bamberger Geographische Schriften **22**: 153-199. – Online abrufbar unter: http://www.uni-bamberg.de/fileadmin/uni/fakultaeten/ggeo_lehrstuehle/geographie_2/Publikationen/Schielein_etal_2007.pdf , 23/02/2011

Schlichting, E., H.-P. Blume und *K. Stahr* 1995: Bodenkundliches Praktikum: Eine Einführung in pedologisches Arbeiten für Ökologen, insbesondere Land- und Forstwirte, und für Geowissenschaftler. – 2. Auflage. – Berlin, Wien

Scicchitano, G., C. Monaco and *L. Tortorici* 2007: Large Boulder Deposits by Tsunami Waves along the Ionian Coast of South-Eastern Sicily (Italy). – Marine Geology **238** (1-4): 75-91

Searle, M. 2006: Co-Seismic Uplift of Coral Reefs along the Western Andaman Islands during the December 26th 2004 Earthquake. – Coral Reefs **25** (1-2): 2

Shaw, B., N.N. Ambraseys, P.C. England, M.A. Floyd, G.J. Gorman, T.F.G. Higham, J.A. Jackson, J.-M. Nocquet, C.C. Pain and *M.D. Piggott* 2008: Eastern Mediterranean Tectonics and Tsunami Hazard Inferred from the AD 365 Earthquake. – Nature Geoscience **1**: 268-276

Shi, S., A. Dawson and *D.E. Smith* 1995: Coastal Sedimentation Associated with the December 12th, 1992 Tsunami in Flores, Indonesia. – Pure and Applied Geophysics (PAGEOPH) **144** (3-4): 525-536

Smedile, A., P.M. De Martini, D. Pantosti, L. Bellucci, P. Del Carlo, L. Gasperini, C. Pirrotta, A. Polonia and *E. Boschi* 2011: Possible Tsunami Signatures from an Integrated Study in the Augusta Bay Offshore (Eastern Sicily, Italy). – Marine Geology, forthcoming

Soloviev, S.L., O.N. Solovieva, C.N. Go, K.S. Kim and *N.A. Shchetnikov* 2000: Tsunamis in the Mediterranean Sea 2000 B.C. – 2000 A.D. – Advances in Natural and Technological Hazards Research **13**. – Dordrecht

Soukissian, T., M. Hatzinaki, G. Korres, A. Papadopoulos, G. Kallos and *E. Anadranistakis* 2007: Wind and Wave Atlas of the Hellenic Seas. – Hellenic Center for Marine Research Publications. – Athens

Tinti, S., A. Maramai and *L. Graziani* 2004: The New Catalogue of Italian Tsunamis. – Natural Hazards **33** (3): 439-465

Tsimplis, M.N. and *A.G.P. Shaw* 2010: Seasonal Sea Level Extremes in the Mediterranean Sea and at the Atlantic European Coasts. – Natural Hazards and Earth System Sciences **10** (7): 1457-1475. – Online available at: http://www.nat-hazards-earth-syst-sci.net/10/1457/2010/nhess-10-1457-2010.pdf, 23/02/2011

Vött, A. 2007: Relative Sea Level Changes and Regional Tectonic Evolution of Seven Coastal Areas in NW Greece since the Mid-Holocene. – Quaternary Science Reviews **26** (7-8): 894-919

Vött, A. und *S.M. May* 2009: Auf den Spuren von Tsunamis im östlichen Mittelmeer. – Geographische Rundschau **61** (12): 42-48

Vött, A., M. May, H. Brückner and *S. Brockmüller* 2006: Sedimentary Evidence of Late Holocene Tsunami Events near Lefkada Island (NW Greece). – In: *Scheffers, A.* and *D. Kelletat*: Tsunamis, Hurricanes and Neotectonics as Driving Mechanisms in Coastal Evolution. – Proceedings of the Bonaire Field Symposium, March 2-6, 2006: A Contribution to IGCP 495. – Zeitschrift für Geomorphologie, Supplement **146**: 139-172

Vött, A., H. Brückner, M. May, F. Lang, R. Herd and *S. Brockmüller* 2008: Strong Tsunami Impact on the Bay of Aghios Nikolaos and Its Environs (NW Greece) during Classical-Hellenistic Times. – Quaternary International **181** (1): 105-122

Vött, A., H. Brückner, S. Brockmüller, M. Handl, S.M. May, K. Gaki-Papanastassiou, R. Herd, F. Lang, H. Maroukian, O. Nelle and *D. Papanastassiou* 2009a: Traces of Holocene Tsunamis across the Sound of Lefkada, NW Greece. – Global and Planetary Change **66** (1-2): 112-128

Vött, A., H. Brückner, S.M. May, D. Sakellariou, O. Nelle, F. Lang, V. Kapsimalis, S. Jahns, R. Herd, M. Handl and *I. Fountoulis* 2009b: The Lake Voulkaria (Akarnania, NW Greece) Palaeoenvironmental Archive – A Sediment Trap for Multiple Tsunami Impact since the Mid-Holocene. – In: *Pavlopoulos, K.* (ed.): Paleo-Evironmental Dynamics and Archaeological Sites. – Zeitschrift für Geomorphologie, Supplement **53** (1): 1-37

Vött, A., G. Bareth, H. Brückner, C. Curdt, I. Fountoulis, R. Grapmayer, H. Hadler, D. Hoffmeister, N. Klasen, F. Lang, P. Masberg, S.M. May, K. Ntageretzis, D. Sakellariou and *T. Willershäuser* 2010: Beachrock-Type Calcarenitic Tsunamites along the Shores of the Eastern Ionian Sea (Western Greece): Case Studies from Akarnania, the Ionian Islands and the Western Peloponnese. – In: *Mastronuzzi, G., H. Brückner, P. Sansò* and *A. Vött* (eds.): Tsunami Fingerprints in Different Archives: Sediments, Dynamics and Modelling Approaches. – Proceedings of the 2nd International Tsunami Field Symposium, September 22-28, 2008, in Ostuni (Italy) and Lefkada (Greece). – Zeitschrift für Geomorphologie, Supplement **54** (3): 1-50

Vött, A., F. Lang, H. Brückner, K. Gaki-Papanastassiou, H. Maroukian, D. Papanastassiou, A. Giannikos, H. Hadler, M. Handl, K. Ntageretzis, T. Willershäuser and *A. Zander* 2011: Sedimentological and Geoarchaeological Evidence of Multiple Tsunamigenic Imprint on the Bay of Palairos-Pogonia (Akarnania, NW Greece). – Quaternary International **242** (1): 213-239

Weindorf, D.C., Y. Zhu, R. Ferrell, N. Rolong, T. Barnett, B.E. Allen, J. Herrero and *W. Hudnall* 2010: Evaluation of Portable X-Ray Fluorescence for Gypsum Quantification in Soils. – Soil Science **174** (10): 556-562. – Online available at: http://ddr.nal.usda.gov/bitstream/10113/37295/1/IND44289200.pdf, 24/02/2011

Yalouris, N. 1957: Δοκιμαστικαί έρευναι είς τόν κόλπον τής Φειάς Ηλείας. – ArchEph **1957**: 31-43

Yalouris, N. 1960: Φειά. – ArchDelt **16/B'**: 126

Yokoyama, I. 1978: The Tsunami Caused by the Prehistoric Eruption of Thera. – In: *Doumas, C.* (ed.): Thera and the Aegean World I: Papers presented at the Second International Scientific Congress, Santorini, Greece, August 1978. – London: 277-283

Zhu, Y. and *D.C. Weindorf* 2010: Determination of Soil Calcium Using Field Portable X-Ray Fluorescence. – Soil Science **174** (3): 151-155

Summary: Olympia's Harbour Site Pheia (Elis, Western Peloponnese, Greece) Destroyed by Tsunami Impact

Geomorphological, sedimentological, geoarchaeological and geochemical investigations were conducted in the environs of ancient Pheia, one of the harbour sites of Olympia (Elis, western Peloponnese, Greece). The studies focused on the Aghios Andreas beachrock and a W-E running vibracore transect across Katakolo Pass. Allochthonous high-energy deposits of marine origin were found repeatedly intersecting autochthonous deposits in terrestrial or quiescent water environments; they represent sedimentary evidence of multiple tsunami landfall. In total, six tsunami generations were discerned. Tsunami deposits were found up to 10 m above present sea level (m a.s.l.) and 650 m inland. Our findings reflect multiple tsunamigenic overflow of Katakolo Pass at 18-20 m a.s.l. Tsunami sediments in the environs of Pheia were found highly complex and variable; associated to erosional unconformities, a number of tsunami-specific sedimentary characteristics were detected such as fining-upward and thinning-inland tendencies, rip-up clasts, lamination, accumulation of marine shell debris, load cast structures and convolute bedding. Ca-Fe ratios of sediment samples based on XRF measurements were used to trace and correlate different tsunami generations. Arguments against interpreting high-energy deposits as storm deposits are discussed. Vibracores and beachrock outcrops document that parts of the tsunami deposits have been post-deposition-

ally cemented to calcarenites. A set of 11 ^{14}C-AMS radiocarbon dates and archaeological age estimations of building remains and ceramic fragments helped to establish a local event-geochronology. The oldest tsunami probably took place already at the beginning of the 6th millennium BC. The major tsunami strike at Pheia was radiocarbon-dated by the sandwich-dating approach to 4300 ± 200 cal BC. Most of the younger events happened in historic times. The tsunami event that finally destroyed the ancient harbour site of Olympia at Pheia was dated to Byzantine to post-Byzantine times. Most probably it occurred in 551 AD associated to an earthquake for which a seismic sea wave is historically attested.

Zusammenfassung: Die Zerstörung von Olympias Hafen Pheia (Elis, Westpeloponnes, Griechenland) durch Tsunami-Impakt

Im Umfeld von Olympias antikem Hafen Pheia (westliche Peloponnes, Griechenland) wurden geomorphologische, sedimentologische, geoarchäologische und geochemische Forschungen durchgeführt. Die Untersuchungen konzentrierten sich auf den Beachrock am Strand von Aghios Andreas und einen W-E verlaufenden Schlaghammerbohr-Transekt über den Pass von Katakolo. Allochthone Hochenergie-Sedimente marinen Ursprungs wurden als wiederholte Einschaltungen in autochthonen Ablagerungen terrestrischer und stillwasserdominierter Ablagerungsräume entdeckt; sie stellen sedimentologische Belege für mehrfache Tsunami-Impakte dar. Insgesamt konnten sechs unterschiedliche Tsunami-Generationen erfasst werden. Tsunami-Ablagerungen wurden bis in eine Höhe von 10 m ü.d.M. und eine Entfernung von 650 m landeinwärts gefunden. Sedimentologische Befunde untermauern eine mehrfache tsunamigene Überströmung des 18-20 m über dem Meer liegenden Passes von Katakolo. Tsunami-Sedimente in der Umgebung von Pheia sind höchst komplex und in ihren Ausprägungen variabel. In Verbindung mit Erosionsdiskordanzen wurden tsunami-spezifische Sedimenteigenschaften wie zum Beispiel fining-upward- und thinning-landward-Tendenzen, rip-up-Klasten, Laminierung, Ansammlung marinen Schills, Belastungsmarken und Wickelschichtung vorgefunden. Mit Hilfe von XRF-Messungen ermittelte Ca-Fe-Verhältnisse von Sedimentproben wurden zum Nachweis und zur Korrelation unterschiedlicher Tsunami-Generationen herangezogen. Argumente gegen die Interpretation der erfassten Hochenergie-Sedimente als Sturmablagerungen werden diskutiert. Die vorliegenden Bohrprofile und das Beachrock-Vorkommen am Strand belegen, dass einzelne Tsunamit-Abschnitte post-depositional zu Kalkareniten verfestigt wurden. Eine lokale Event-Geochronologie konnte mit Hilfe von 11 ^{14}C-AMS-Radiokohlenstoffdatierungen sowie der archäologischen Altersbestimmung von Bauresten und Keramikfragmenten erstellt werden. Der älteste Tsunami ereignete sich wahrscheinlich bereits zu Beginn des 6. Jahrtausends v. Chr. Das stärkste Tsunami-Ereignis, welches Pheia erfasste, konnte mittels ^{14}C-AMS-Datierungen im Sandwich-Verfahren auf 4300 ± 200 cal v. Chr. datiert werden. Die meisten jüngeren Tsunamis ereigneten sich in historischer Zeit. Der Tsunami, der den antiken Hafen von Olympia bei Pheia schließlich zerstörte, fand in byzantinischer bis post-byzantinischer Zeit statt. Höchstwahrscheinlich ereignete er sich im Jahr 551 n. Chr. im Zusammenhang mit einem Erdbeben, für welches das Auftreten einer seismischen Woge historisch überliefert ist.

Résumé: La destruction de Pheia – le port d'Olympie – (Elis, Péloponnèse de l'ouest, Grèce) par l'impact d'un tsunami

Des investigations géomorphologiques, sédimentologiques, géoarchaéologiques et géochimiques étaient réalisées aux environs de l'ancien Pheia, le port d'Olympie (Elis, Péloponnèse de l'ouest, Grèce). Les études scientifiques s'étaient concentrées sur le beachrock d'Aghios Andreas et le long d'un profil de carottages à travers le Col de Katakolo courant d'une direction ouest-est. Nous avons trouvé des interférences répétées de sédiments allochtones d'haute énergie et d'origine marine au sein des sédiments autochtones qui étaient accumulés dans des environnements terrigènes ou lacustrines, ces interférences faisant preuve d'impact multiple de nature tsunamigène. En total, six générations de tsunami ont été découvertes. Des dépôts tsunamigéniques ont été trouvés jusqu'à 10 m au-dessus du niveau de la mer et jusqu'à 650 m éloigné du bord de

la mer. Nos résultats témoignent l'inondation répétée du Col de Katakolo situé à 18-20 m au-dessus du niveau de la mer par tsunami. Les dépôts tsunamigéniques trouvés aux environs de Pheia sont très complexes et variables. Nombreuses propriétés sédimentaires caractéristiques pour tsunamis ont été trouvées rattachées à des contacts d'érosion, par exemple *fining upward*, *thinning landward*, *rip-up clasts*, stratification, débris de coquillages, *load cast* et *convolute bedding*. Des relations entre Ca et Fe trouvées pour des échantillons de sédiment par mesurages à XRF ont été utilisées de percevoir et corréler les générations différentes de tsunami. De plus, des arguments contre l'interprétation des sédiments d'haute-énergie comme dépôts de tempête sont discutés. Les carottages et l'affleurement du beachrock documentent que des parties intérieures des dépôts tsunamigéniques ont été cémentées au cours d'une phase post-sédimentaire comme calcarénite. Au moyen d'onze datations de radiocarbone ^{14}C-AMS et de la détermination de l'âge de restes de bâtiment et de fragments de céramique, il était possible d'établir une géochronologie locale des événements. Le tsunami le plus aîné a eu lieu au commencement du sixième millénaire avant Jésus-Christ. L'impact le plus fort à Pheia était daté par la méthode radiocarbone à sandwich à 4300 ± 200 cal av. J.-C. La plupart des événements plus jeunes ont pris place au fil de l'époque historique. Le tsunami qui a finalement démolit l'ancien port d'Olympie à Pheia était daté au temps byzantin à post-byzantin. Il est probable que ce tsunami s'est passé en 551 AD parce qu'un raz de mer est attesté pour cette année par des sources historiques.

Prof. Dr. Andreas Vött, Dipl.-Geogr. Hanna Hadler, Dipl.-Geogr. Konstantin Ntageretzis, Dipl.-Geogr. Timo Willershäuser, Geographisches Institut, Johannes-Gutenberg-Universität, Johann-Joachim-Becher-Weg 21, 55099 Mainz, Germany, voett@uni-mainz.de, hadler@uni-mainz.de, konstantin.ntagaretzis@uni-mainz.de, timo.willershaeuser@uni-mainz.de

Prof. Dr. Georg Bareth, Prof. Dr. Helmut Brückner, Geographisches Institut, Universität zu Köln, Albertus-Magnus-Platz, 50923 Köln, Germany, g.bareth@uni-koeln.de, h.brueckner@uni-koeln.de

Prof. Dr. Franziska Lang, Fachgebiet Klassische Archäologie, Technische Universität Darmstadt, El-Lissitzky-Str. 1, 64287 Darmstadt, Germany, flang@klarch.tu-darmstadt.de

Dr. Dimitris Sakellariou, Hellenic Centre for Marine Research (HCMR), 47th km, Athens-Sounio Ave., 19013 Anavyssos, Greece, sakell@ath.hcmr.gr

Manuscript submitted: 03/08/2010
Accepted for publication: 29/01/2011